Bioresource Technology 447 (2026) 134217

Contents lists available at ScienceDirect

Bioresource Technology

journal homepage: www.elsevier.com/locate/biortech

Development of a bioprocess with *Streptomyces setonensis* to produce a novel herbicidal sugar as an alternative to glyphosate

X. Steurer [a,*], B. Kalik [a,b], D. Jakobs-Schönwandt [a,c], A. Grünberger [d], A.V. Patel [a,*]

[a] University of Applied Sciences and Arts Bielefeld (HSBI), Bielefeld Institute of Applied Materials Research, Fermentation and Formulation of Biologicals and Chemicals, Interaktion 1, 33619 Bielefeld, Germany
[b] University Bielefeld, Faculty of Technology, Universitätsstrasse 25, 33615 Bielefeld, Germany
[c] Westphalian University of Applied Sciences, Campus Recklinghausen, Faculty of Engineering and Natural Sciences, Bioengineering and Sustainability, August-Schmidt-Ring 10, 45665 Recklinghausen, Germany
[d] Karlsruhe Institute of Technology, Faculty of Chemical and Process Engineering, Microsystems in Bioprocess Engineering, Kaiserstraße 12, 76131 Karlsruhe, Germany

HIGHLIGHTS

- Production of the herbicidal sugar 7-deoxy-sedoheptulose with a wildtype *Streptomyces*.
- Systematic bioprocess development by DOE and RAMOS® for metabolism insights.
- Elevated osmolarity and phosphate quantity as key factors for increased 7dSh production.
- Glucose feeding strategy enhanced the 7dSh titer by a factor of 200 to 4.5 g/L.
- Constant power input (P/V) as successful scaling strategy to a 15 L stirred-tank reactor.

GRAPHICAL ABSTRACT

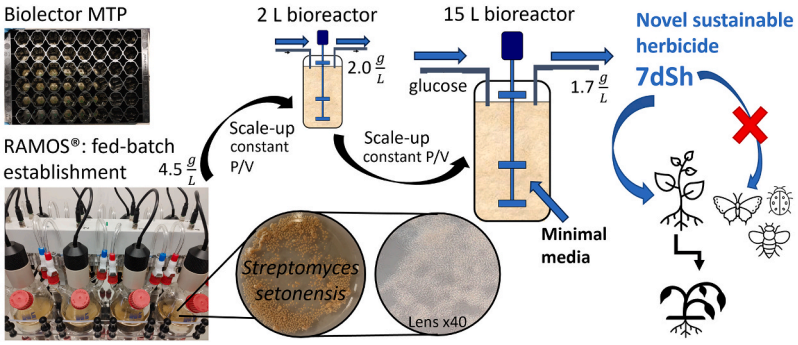

ARTICLE INFO

Keywords:
Bioprocess development and optimization
Online-monitoring
Design of experiments (DOE)
7-Deoxy-sedoheptulose
Sustainable agriculture

ABSTRACT

The controversial herbicide glyphosate is widely applied to reduce weeds worldwide, to increase agricultural yields to feed the world's population. Emerging plant resistances and its negative impact on the environment and living beings urge for an effective as well as ecologically acceptable alternative. *Streptomyces setonensis,* a natural producer strain of such a novel herbicidal substance, seems a promising biocatalyst for the large-scale production of 7–deoxy–sedoheptulose (7dSh). However, this strain has been marginally investigated. Therefore, we developed a microbial production process for 7dSh, systematically optimizing it by investigating essential factors such as medium composition, phosphate and nitrogen limitation, as well as process parameters and modes. Starting on a small scale, the experiments were conducted in a high throughput microbioreactor system (BioLector), in shake flasks employing a Design of Experiments approach and complemented by real–time oxygen transfer measurements with RAMOS® (Respiration Activity MOnitoring System) to gain a deeper understanding of the bacterial metabolism. Elevated osmolarity emerged as a critical factor for 7dSh production. Surprisingly, increased phosphate concentrations enabled an altered metabolism after the growth phase and extended culture longevity, allowing for the application of a feeding strategy. The optimized process was successfully scaled up to a 15 L

* Corresponding authors at: University of Applied Sciences and Arts Bielefeld (HSBI), Interaktion 1, 33619 Bielefeld, Germany.
E-mail addresses: xenia_ricarda.steurer@hsbi.de (X. Steurer), Desiree.Jakobs-Schoenwandt@w-hs.de (D. Jakobs-Schönwandt), alexander.gruenberger@kit.edu (A. Grünberger), anant.patel@hsbi.de (A.V. Patel).

https://doi.org/10.1016/j.biortech.2026.134217
Received 17 December 2025; Received in revised form 10 February 2026; Accepted 11 February 2026
Available online 14 February 2026

stirred tank bioreactor. Ultimately, a 200–fold increase in 7dSh titer from 22 mg/L to over 4 g/L was achieved. This represents the highest reported concentration to date and provides a solid foundation for pilot–scale production. The obtained titers pave the way for downstream formulation studies to establish 7dSh as a sustainable herbicide in modern agriculture.

1. Introduction

Weeds pose a severe threat to agricultural yields and to areas used for settlement and transport. To reduce food loss and ensure sufficient food supply for the growing global population, the use of herbicides has increased strongly worldwide [Mohd Ghazi et al., 2023; Sparks and Lorsbach, 2016]. Currently, the globally most applied herbicide is glyphosate, followed by 2,4–dichlorophenoxyacetic acid and atrazine, which reduce the growth of undesired plants [Duke and Powles, 2008; Mohd Ghazi et al., 2023]. However, intensive application has led to the accumulation of pesticides and their degradation products in the environment [Mohd Ghazi et al., 2023; Soares et al., 2021]. Glyphosate in particular has been detected in soil, surface water, groundwater, sediments, food, animals and humans, sparking a controversial debate [Battaglin et al., 2014; Gandhi et al., 2021; Rawat et al., 2023; Soares et al., 2021; Wang et al., 2016]. Various studies have demonstrated the negative effects of glyphosate and its formulations on insects [Farina et al., 2019; Kiefer et al., 2021; Smith et al., 2021], aquatic organisms [Klátyik et al., 2024] and microbial communities, exerting a systemic negative influence on ecosystems and the environment [Pérez et al., 2011; Rawat et al., 2023; Ruuskanen et al., 2022]. Concerns have also been raised about glyphosate's toxicity and carcinogenicity in humans [Gandhi et al., 2021; Meftaul et al., 2020]. Therefore, an effective and ecologically acceptable alternative is urgently needed.

The hazards posed by herbicidal chemicals and their degradation products are not the only concern. Repeated applications of commercially available herbicides, such as non–triazine, low-use-rate sulfonylurea and imidazolinone herbicides, have steadily raised the number of resistant weed biotypes [Knezevic et al., 2016; LeBaron and Hill, 2008; Lovell et al. 1996]. Hence, these plants require evolved control agents [Duke and Powles, 2009; LeBaron and Hill, 2008], but the development and marketing of herbicides with new modes of action have been slow and challenging in recent years [Duke et al., 2018; He et al., 2022]. The application of increasing amounts and combinations of herbicides for the protection of crop yields results in a spiral of resistance and environmental damage [Busi et al., 2013; Gandini et al., 2020; Parven et al., 2024]. A promising alternative to replace harmful or inefficient agents are novel herbicidal substances that target pathways in plants which cannot be bypassed and arrest growth or cause cell death without harmful side effects on non–target organisms [Brilisauer et al., 2019].

7–Deoxy–sedoheptulose (7dSh) is such a novel herbicidal candidate. This sugar was first isolated from stationary phase culture supernatants of *Synechococcus elongatus* and inhibits the growth of other cyanobacteria in a dose-dependent manner [Brilisauer et al., 2019]. As no effect of 7dSh could be demonstrated on *Gluconobacter oxydans* as a representative for bacteria, an effect on photosynthesis was hypothesized. Further investigation revealed that 7dSh affects anabolic reactions, leading to the accumulation of 3–deoxy–D–*arabino*-heptulosonate-7–phosphate (DAHP) in *Anabaena variabilis*, another cyanobacterium [Brilisauer et al., 2019]. This molecule is metabolized by the second enzyme of the shikimate pathway. As 7dSh interferes with this pathway which generates aromatic amino acids in bacteria, fungi and plants, but not in animals, analogous to glyphosate [Duke and Powles, 2008], its herbicidal effects were investigated [Brilisauer et al., 2019]. Indeed, 7dSh had a detrimental impact on the germination and growth of *Arabidopsis thaliana* seedlings, resulting in reduced size, smaller roots and fewer root hairs, to a greater extent than glyphosate at the same concentration [Brilisauer et al., 2019]. To ensure the safe application of 7dSh as a herbicide, initial studies excluded cytotoxicity on different human cell lines and adverse effects on the embryonic development of zebrafish [Brilisauer et al., 2019; Schweizer et al., 2019].

According to scholarly literature, there are several ways to produce 7dSh. The chemoenzymatic synthesis process for 7dSh with the recombinantly expressed and purified transketolase from *S. elongatus* and the high-cost substrates 5–deoxy–D–ribose and β–hydroxypyruvate has a yield of 20 % [Brilisauer et al., 2019]. During a 30–days cultivation of *S. elongatus* with 2 % CO_2-supplemented air, 7 μM (1.3 mg/L) of 7dSh were produced in a special salvage pathway for 5–deoxyadenosine, which is processed to 5–deoxyribose and further to 7dSh by promiscuous enzymes [Rapp et al., 2021]. Thereby, the promiscuous transketolase exhibits a 100–fold higher affinity for its natural substrate, D–ribose–5–phosphate, than for 5–Deoxyribose [Brilisauer et al., 2019]. In general, processes involving cyanobacteria have attracted the attention of researchers because atmospheric CO_2 can be exploited as a carbon source, thus avoiding competition with food and feed stocks, while sunlight serves as an energy source to produce green fine – and platform chemicals and fuels [Carroll et al., 2018]. However, biotechnological processes with non-engineered cyanobacteria present challenges due to low yields and concentrations, insufficient carbon fixation efficiency, and high susceptibility to produced chemicals [Kanno et al., 2017; Lai et al., 2022; Pressley et al., 2024; Tan et al., 2022]. Even engineered cyanobacteria are frequently outperformed by modified *E. coli* in terms of titer [Liu et al., 2022]. In contrast, industrial processes involving different *Streptomyces* strains to produce antibiotics are common practice [Barka et al., 2016; Hopwood 2007; van Wezel et al., 2006]. The compound SF-666, naturally produced by *Streptomyces setonensis*, was first described by Ezaki et al. [1970] and was demonstrated to be identical to 7dSh from *Synechococcus elongatus* by Brilisauer et al. [2019]. *S. setonensis* produced 113 μM (22 mg/L) of 7dSh after 7 days of cultivation in complex media, whereby 7dSh is secreted to the culture supernatant [Rapp et al., 2021]. This is 16 times the concentration *S. elongatus* forms. However, this strain has been studied poorly so far. Since its genome sequence is not yet published, the gene locus for 7dSh production remains unknown. Only some basic investigations were conducted in the 1970s, describing growth temperature and behaviour on different solid agar media and carbon sources [Shomura et al., 1970]. This lack of research in combination with the great potential of *S. setonensis* shows the importance of studying its needs and optimising its cultivation conditions. Process parameters and media composition are known to influence the biotechnological production of value-added products, but the ideal combination of the parameters differs for each process and organism [Bundale et al., 2015; Ferraiuolo et al., 2021; López-García et al., 2014]. To circumvent this problem, work has been done in synthetic biology to design a universal biocatalyst [Davy et al., 2017; Guan et al., 2024; Rosch et al., 2024; Shi et al., 2022]. However, the approval process for biopesticides is highly regulated, time-consuming and costly and becomes even more complicated when genetically modified organisms are used in the production process [Desai et al., 2016; Montesinos, 2003]. Thus, there is still a frequent need for efficient, structured bioprocess development with wildtype strains.

In this study we developed a novel bioprocess for 7dSh production as an alternative herbicide with *S. setonensis* for the first time. First, we investigated key factors such as medium composition and process parameters on a small scale in a high throughput microbioreactor system (BioLector) and in shake flasks using a Design of Experiments (DOE) approach to identify optimal conditions for growth and production. Thereby, we hypothesized that exerting osmotic stress may alter genetic

expression and trigger a metabolic shift towards a higher 7dSh production. Furthermore, consistent with the filamentous growth morphology of *S. setonensis*, we expect advantages of protecting the organism from shear stress rather than enabling high oxygen transfer rates. To systematically optimize the process and to gain a deeper understanding of the bacterial metabolism, we conducted real-time oxygen transfer measurements with RAMOS® (Respiration Activity MOnitoring System) while investigating process modes and phosphate and nitrogen limitation. These are considered to benefit secondary metabolite production in other *Streptomyces* species. Finally, we scaled up beneficial culture conditions identified at the small scale to a 2 L bioreactor approach and subsequently to a 15 L bioreactor, laying the foundation for large-scale 7dSh production.

2. Materials and methods

2.1. Strain and inoculum preparation

The strain of *S. setonensis* used in this study was kindly provided by Prof. Dr. Forchhammer's working group at the University of Tübingen and by the Research Laboratories of MeGi Seika Kaisha Ltd. in Morooka, Yokohama, Japan.

The strain maintenance and preparation of *S. setonensis* spore solutions are described by Shepherd et al. [2010] in Basic Protocol 5. The strain was grown for 7 to 10 days at 28 °C to stimulate spore formation on soy-mannitol-agar plates (containing per L 20 g mannitol, 20 g soya bean flour, 16 g agar) [Hobbs et al., 1989]. Spores were harvested by scrubbing the plates with a spatula and suspending the spores in 3 mL of sterile deionised water. After transferring the liquid from the plates to a 50 mL falcon tube and mix vigorously, the solution was filtered through an autoclaved falcon with cotton fabric and a cut hole in the bottom and then washed. The filtered spore solution was then centrifuged for 10 min at 4500 rpm and 4 °C (Hettich Rotixa 50 RS), after which the supernatant was discarded, leaving 2 mL of residual solution in which the spores were diluted 1:1 with a 50 % (v/v) glycerol solution. Aliquots were stored at –32 °C. The concentration of the spore solution was determined by plating a dilution series on potato extract glucose agar (39 g/L; Carl Roth) and counting colony forming units (CFU).

2.2. Media

The basic minimal medium proposed by Koepff et al. [2018] was adapted and contains the following: 25 g/L D–glucose monohydrate, 11.7 g/L NaCl (as proposed by Hobbs et al. [1989]), 2.07 g/L NaH_2PO_4xH_2O, 2.6 g/L K_2HPO_4, 3 g/L $(NH_4)_2SO_4$, 0.56 g/L $MgSO_4 \cdot H_2O$, 19.5 g/L 2–(N–morpholino)ethanesulfonic acid (MES) buffer. The pH was adjusted to a value of 7 with NaOH. Before cultivation, the autoclaved stock solution was supplemented with the separately autoclaved concentrated glucose and magnesium sulphate solutions, as well as with a sterile filtered trace elements solution combining the trace salts of Koepff et al. [2018] and Hobbs et al. [1989]. The trace elements solution – concentrated by a factor of 1000 – contains 10 g $ZnSO_4$, 8.775 g $FeCl_3$, 2 g $ZnSO_4$x$6H_2O$, 1 g $CaCl_2$, 1 g $MnCl_2$xH_20, 1 g $FeSO_4$x$7H_2O$, 0.425 g $CuCl_2$x$6H_20$, 0.415 g KI, 0.31 g H_3BO_3, 0.242 g Na_2MoO_4x$2H_20$. The medium composition varied as indicated in the Results section in the respective figure captions. The detailed compositions are provided in Appendix Table S1.

2.3. Shake flask experiments – Design of experiments

Process key parameters were investigated by means of a DOE approach in shake flask cultivations for 10 days at 28 °C on a shaker (IKA KS 4000i control). The flasks with a nominal volume of 300 mL were inoculated with $2.7 \cdot 10^6$ CFU from a cryo spore solution. Samples for offline analytics were taken after 6, 8 and 10 days, biomass dry weight was determined after harvest. A fractional factorial design, resolution III, linear model was chosen with 5 factors at two levels (filling volume, shaking speed, osmolarity and concentration of carbon source (C source) and nitrogen source (N source)) and one response (7dSh titer), resulting in 8 boundary point experiments (n = 3; see Appendix Table S2). The software Minitab (Minitab Statistical Software) was employed for the evaluation and interpretation of the results. The ranges were carefully chosen to generate effects while staying within the boundaries in which growth is supported, by consulting literature of other *Streptomyces* processes. Carbon catabolite and nitrogen metabolite regulation are known to influence secondary metabolite production in *Streptomyces* [Liu et al., 2013; Martin and Demain 1980; Romero-Rodríguez et al., 2018]. In some cases, glucose, as the favored carbon source for growth, leads to the repression of antibiotic production [Martin and Demain, 1980], whereas a metabolic switch induces antibiotic synthesis if glucose is the less favored carbon source [Kominek, 1972]. When quickly utilizable organic or inorganic nitrogen sources are present, repression of secondary metabolite production has been shown [Hobbs et al., 1992; Doull and Vining 1990; Aharonowitz and Demain, 1979]. Therefore, the C source (glucose) varied from 10 g/L in the minimal medium used by Koepff et al. [2018] to 25 g/L in the complex medium supplemented by Brilisauer et al. [2019]. The N source (ammonium sulphate) varied from 3 g/L [Koepff et al., 2018] to 7.5 g/L, corresponding to the molar amount of 4.5 g/L $NaNO_3$ employed by Hobbs et al. [1989]. The osmolarity (Osm) varied due to differences in the concentration of the C and N source and further due to NaCl addition between 0 M [Koepff et al. 2018] and 0.2 M. This corresponds to a medium amount of ionic osmolytes to remain below the concentration of 0.5 M NaCl, causing osmotic shock in *S. coelicolor* [Fuchino et al., 2017], of 0.6 M NaCl, inducing adverse effects on morphology with regard to size and cell wall integrity in *S. venezuelae* and *K. viridifaciens* [Ramijan et al., 2018] and of 1 M NaCl that arrests growth in marine *Streptomyces* strains [Ameur et al., 2011]. The influence of oxygen transfer rate (OTR) and shear stress on biosynthesis has been demonstrated in a stirred tank bioreactor (STR) and in wave-mixing bioreactors for *S. clavuligerus* [Gómez-Ríos et al. 2019; Ribeiro et al. 2021]. Both parameters are affected by filling volume and shaking speed in shaken bioreactors [Maier and Büchs, 2001; Giese et al., 2014]. The filling volume varied from 18 to 49 mL, corresponding to 6 and 16 % of the nominal flask volume, which is within the range of commonly investigated filling volumes [Anderlei et al., 2004; Guez et al., 2008]. The shaking speed was set to 140 or 180 rpm to avoid adverse effects of shear stress on mycelium viability [Zacchetti et al., 2018; López-García et al., 2014]. These ranges also include lower maximum oxygen transfer capacities [Meier et al., 2016], because effects of hypoxia on secondary metabolism have been observed [Gallagher et al., 2017].

2.4. Shake flask experiments – respiration activity MOnitoring system

Metabolic activity can be determined by online monitoring of the OTR during the cultivation and biological phenomena such as substrate or oxygen limitation, product inhibition and diauxic growth can be identified by their characteristic OTR curves [Anderlei and Büchs, 2001]. Fast growing organisms encounter oxygen supply issues at higher filling volumes or lower shaking speeds, with OTR_{max} being reached within 20 h [Wewetzer et al., 2015]. In the case of *S. lividans*, it has been demonstrated that antibiotic production increases at low oxygen levels in normal shake flasks compared to baffled ones [Gamboa-Suasnavart et al., 2018]. To gain a deeper understanding of the metabolism and to verify the influence of oxygen availability on 7dSh production, we measured the oxygen uptake via the OTR [Anderlei and Büchs, 2001; Anderlei et al., 2004]. Therefore, further shake flask cultivations were performed with a Respiration Activity MOnitoring System (RAMOS®, HiTec Zang) in 250 mL flasks at 30 °C, 130 rpm, with a filling volume of 33 mL and a shaking diameter of 50 mm. Monitored flasks and additional unmonitored shake flaks were run in duplicates, triplicates or quadruplicates, as stated in the results section. Supernatant samples

ranging from 0.3 to 1 mL were taken regularly. Flasks were inoculated with $6 \cdot 10^6$ CFU from a cryo spore solution.

In actinomycetes secondary metabolites are typically produced following the rapid growth phase, when one or more nutrients become growth-limiting, so that the growth rate drops below a certain level [Martin and Demain, 1980]. The transition between the phases is often not sharply delimited, resulting in continued cell dry weight increase, but one indicator is a decrease in respiratory activity [Martin and McDaniel, 1975]. Moreover, regulatory mechanisms additionally influence particular biosynthetic pathways in different ways [Martin and Demain, 1980; Liu et al., 2013]. Phosphate limitation has been reported to have a positive influence on biocatalysis in *Streptomyces* strains, as this limitation triggers a switch in metabolism to the synthesis of antibiotics and other secondary metabolites [Martin, 2004]. The source and availability of nitrogen affect metabolic regulation and influence primary and secondary metabolism, while being interconnected with the usage of phosphate and carbon [Romero-Rodríguez et al., 2018]. As nitrogen-limiting concentration, 5 mM Na–nitrate or 7.5 mM of ammonium were considered [Tiffert et al., 2008; Novák et al., 1992]. Glucose is a preferred carbon source in *Streptomyces*, but depending on the concentration, transcription of secondary metabolite clusters is downregulated and interference with morphological differentiation has been demonstrated [Romero-Rodríguez et al., 2018]. Dzhavakhiya et al. [2016], Elsayed et al. [2015], Gómez-Ríos et al. [2022] and Wallace et al. [1996] employed a fed-batch mode in different *Streptomyces* strains to overcome catabolite repression and enhance the production of antibiotics and secondary metabolites. Therefore, we investigate in the RAMOS® experiments additionally phosphate excess and limitation, different nitrogen sources and nitrogen addition during cultivation, as well as glucose feeding after the growth phase. Feeding was executed from feed bottles with an air filter (PTFE, 0.2 µm, Carl Roth) via tubes (silicone 1.5 x 3.5 mm and TPV 0.8 x 4 mm) with a sterile filter (Cellulose acetate, 0.2 µm, Carl Roth) and a disposable needle (Sterican 0.55 x 25 mm, B. Braun) through a septum (silicone rubber GL25, DWK) to the sampling port of the RAMOS® flasks. Pressure was applied via a peristaltic pump (L100-1S-2 DG-8–6, Longer).

2.5. Microtiter plate experiments

A high-throughput microbioreactor system (BioLector Pro, Beckman Coulter, former m2p-labs) was employed for 48 well microtiter flower plate experiments (pH/DO type 2 LG1/RF; M2P-MTP-48-BOH2, Beckman). The system allows for online monitoring of biomass growth by scattered light (Gain 1;7) and of pH (4.8 – 7.2; LG1; Ex 508 nm/ Em 550 nm) and dissolved oxygen (RF; Ex 620 nm/ Em 775 nm) by excitation of special polymers in optodes in the bottom of each well and detection of the reflected fluorescence. In this way valuable complementary data to RAMOS® shake flasks experiments is provided, facilitating faster and more advanced bioprocess development through the exploration of a wider variety of parallel treatments in biological triplicates [Wewetzer et al. 2015]. The shaking frequency was set to 800 rpm, the filling volume was 1.2 mL, and each well was inoculated with $5.3x10^5$ CFU from a cryo spore solution. The plate was sealed with an evaporation limiting foil (M2P-F-GPR48-10, Beckman), acting as a sterility barrier and the incubation chamber was held at 30 °C with 75 % humidity. After 7 days, a 200 µL sample was taken from each well, filtered immediately, and stored at –32 °C. After 10 days of cultivation, the remaining supernatant was stored as a sample.

2.6. Scale-up

To scale up the process to a stirred tank bioreactor, a decision is required on which key criteria should be kept constant [Marques et al., 2010; de Souza et al., 2022]. The first scale-up is from 250 mL shake flasks to a baffled stirred tank bioreactor (STR; Biostat B Plus, Sartorius Stedim, total volume 3 L) equipped with two 6–bladed dual Rushton turbines with a filling volume of 2 L and a maximum aeration rate of 2 vvm. The stirring rate of the bioreactor was calculated by choosing to keep the volumetric power input constant. The volumetric power input in the 250 mL shake flasks with a filling volume V_L of 0.033 L and with an inner diameter d of 0.075 m at a stirring rate n of 130 rpm was calculated by using the empirical constant $C_3 = 1.94$ and the following formula according to Büchs et al. [2000]:

$$\frac{P}{V_L} = C_3 \cdot \frac{\rho \cdot n^3 \cdot d^4}{V_L^{2/3}} \cdot Re^{-0.2} \quad (1)$$

Thereby the Reynolds number Re is calculated with $D_R = d$ according to this formula [Rushton, 1950]:

$$Re = \frac{\rho}{\eta} \cdot n \cdot {D_R}^2 \quad (2)$$

The density of the culture broth is measured with a hydrometer, resulting in a value of $\rho = 1.026$ kg/m^3 and the dynamic viscosity η is estimated using the viscosity of a 2 % glucose solution at 20 °C, which is 1.052 mPa·s [Wolf, 1966; Söhnel and Novotny, 1985]. This results in Re $= 1.19 \cdot 10^4$ for the shake flasks.

The volumetric power input (P/V) results in 95.3 W/m^3. Therefore, when kept constant, the power input in the 2 L bioreactor results in 0.19 W. For an aerated system, the relation of gassed power input P_g to ungassed power input P is defined by the empirical formulas published by Cui et al. [1996]:

$$\frac{Q_g \cdot n^{0.25}}{{D_R}^2} \leq 0.055 \qquad 1 - \frac{P_g}{P} = 9.9 \cdot \left(\frac{Q_g \cdot n^{0.25}}{{D_R}^2}\right) \quad (3)$$

$$\frac{Q_g \cdot n^{0.25}}{{D_R}^2} > 0.055 \qquad 1 - \frac{P_g}{P} = 0.52 + 0.62 \cdot \left(\frac{Q_g \cdot n^{0.25}}{{D_R}^2}\right) \quad (4)$$

Thereby, the volumetric air flow rate Q is $6.66 \cdot 10^{-5}$ m^3/s, giving a $Q_g n^{0.25} D_R{}^{-2}$ of 0.034 for the 2 L reactor. Therefore, with a value of 0.19 W for P_g and a starting value for n of 250 rpm [Dzhavakhiya et al., 2016], P for both stirrers is calculated using equation (eq.) (3), which results in a value of 0.287 W. P is defined by the following formula [Kracík and Moucha, 2021]:

$$P = Ne \cdot \rho \cdot n^3 \cdot {D_R}^5 \quad (5)$$

Thereby, the stirrer diameter D_R is 0.053 m. The Newton number Ne, also known as the power number, is published for various systems and remains constant as long as turbulent flow regimes can be assumed by Re $> 10^4$ [Kaiser et al. 2018]. The power number of a dual impeller system is approximately twice that of a single impeller, when the spacing between the impellers is greater than $2D_R$ [Hudcova et al., 1989; Bates et al., 1963]. The spacing between the two Rushton turbines is with 9 cm slightly lower than $2D_R$ (=10.6 cm), thus, to compensate for a weak interaction between the two impellers during creating the flow regime, the experimentally determined Ne = 8.9 for dual Rushton turbines of Taghavi et al. [2011] is used. With Ne and P, the stirring speed is then calculated by solving eq. (5) for n, resulting in a value of 253 rpm, which is rounded off to 250 rpm, thus affirming the starting value applied for the calculation with eq. (3). Subsequently, the Reynolds number Re $= 1.14 \cdot 10^4$ for the 2 L bioreactor is calculated using eq. (2), which confirms that the assumption of turbulent flow regimes and therefore constant Ne was correct.

For the next scale-up step to a 15 L bioreactor, several dimensionless numbers were considered and calculated, including the Newton and Reynolds number (see above), the oxygen volumetric mass transfer coefficient (k_La) was measured (see 2.8) and as for the 2 L reactor as scaling strategy the volumetric power input [Garcia-Ochoa and Gomez 2008; Marques et al., 2010; Stanbury et al., 2016] was chosen to be kept constant.

With n = 250 rpm = 4.16 s^{-1} and eq. (5) P results in a value of 0.276

W and with eq. (3) P_g in a value of 0.184 W. Hence, the volumetric power input is 91.8 W/m^3. When the volumetric power input is kept constant during scale-up, the gassed power input to the 15 L reactor results in P_g = 1.376 W. To calculate the unaerated power input, a starting value for the iterative solution of the speed n is required, so that the minimal n (n_{min}) for a turbulent flow regime is determined according to Peter [2006]:

$$n_{min} = \frac{\nu}{\pi \cdot D_R \cdot h_1} \cdot \sqrt[3]{\frac{200^4}{c_D \cdot 0.4^4}} \quad (6)$$

For the 15 L reactor $D_R = 0.07$ m and the stirrer height $h_1 = 0.014$ m; n_{min} is therefore calculated with the kinematic viscosity $\nu = \eta/\rho$ [m^2/s] and the dissipation coefficient c_D = 0.1 with eq. (6), resulting in 2.84 s^{-1}. With Q = 0.00025 m^3/s and n_{min}, $Q_g n^{0.25} D_R^{-2}$ results in 0.066, thus, eq. (4) is valid, and the relation of P_g to P yields 0.439. This results in an unaerated power input of 3.14 W. Thus, the power input for each of the three 6–bladed Rushton turbines is 1.05 W. With Ne = 5.5 [Kracík and Moucha 2021], and iterative solving of eq. (4) and (5) for power input and speed, n = 289 rpm is obtained for the stirring speed at the larger scale.

At the larger scale, Re is $2.30 \cdot 10^4$, which is twice as high as at the smaller scale. The higher Re aligns with other successful scale-up processes [Marques et al., 2010]. In terms of the geometric similarity of the vessels [Yang et al., 2007], the ratio of the stirrer diameter to the reactor diameter (53/130 mm and 70/200 mm, resulting in 0.41 and 0.35, respectively) and the ratio of the stirrer blade height to the stirrer diameter (0.19 and 0.2, respectively) remain within the same range. The filling height increases from 0.175 m to 0.4 m, and the bottom clearance of the stirrer increases from 0.045 m to 0.102 m. Consequently, the ratio of these dimensions to the stirrer diameter also increases. As the geometry of the reactors was fixed, changes to these dimensionless numbers were unavoidable. The measured and calculated reactor parameters and dimensionless numbers are summarized in Appendix Table S4.

2.7. Stirred tank bioreactor cultivations

Fermentations in the 2 L bioreactor were performed in duplicate in batch, repeated batch and fed-batch modes. The conditions for performing the bioprocess in the 2 L bioreactor were adapted from those used for production processes with other *Streptomyces* strains [Dzhavakhiya et al., 2016; Large et al., 1998; Zhou et al., 2018]. The total filling volume was 2 L and the temperature was controlled at 28 °C. Aeration was increased from 1 vvm to 2 vvm as soon as the dissolved oxygen tension (DOT) fell below 20 %. The stirring speed was set to 250 rpm (see 2.6). The pre-culture in 250 mL shake flasks, with a filling volume of 35 mL of standard medium, was inoculated with 4x10^6 CFU from a cryo spore solution and grown for 7 days at 28 °C and 150 rpm on a shaker (IKA KS 4000i control). Each reactor was inoculated with the pooled cell pellets from three pre-culture shake flasks, without supernatant, suspended in 200 mL of fresh medium via peristaltic pumping through an inlet nozzle. To prevent foaming, 0.2 to 0.3 mL of sterile filtered Pluronic PE 8100 (BASF) were added at the start of the fermentation. The pH was controlled at 7 by adding 2 M NaOH or 2 M HCl as required. For the fed-batch process, cultivation began with a filling volume of 1.7 L. After 69 h or 72 h feeding commenced at a rate of 5.1 mL/h via a peristaltic pump (Ismatec ISM831C) with a silicone hose (Rotilabo, Carl Roth, 3 mm diameter) connected to an inlet nozzle. The 0.3 L feeding solution contained either 61 g/L or 122 g/L glucose, as indicated in 3.4, as well as the necessary medium salts to maintain the initial concentration of each component and prevent the culture medium from being diluted by the feed. Samples were taken from the reactors once or twice a day via a 3–way sampling bottle.

The stirring speed for the process in the 19 L NLF reactor (Bioengineering, NLF 1) with a filling volume of 15 L was set to 290 rpm (see 2.6). The other process parameters were adopted from the 2 L cultivation. The 15 L process run at 28 °C, with an aeration rate of 1 vvm, an overpressure of 0.2 bar, pH control at 7 with 2 M NaOH and 2 M phosphoric acid and automatic foam control with Pluronic PE 8100. For inoculation of the larger bioreactor, the 2 L reactor served as seed fermenter, which was inoculated as in the batch process described above. The seed batch process reached a biomass dry weight of 5.2 g/L in 66 h. The cells were harvested sterile, sedimented and the supernatant was discarded. Then, the cells were resuspended in 1 L of fresh medium and transferred to the 19 L NLF reactor by pressurized air. The 0.85 L feeding solution contained 465 g/L glucose, corresponding to the extrapolated glucose consumption rate, and was pumped via the hose pump of the reactor control unit with a cycle of 10 s pumping at 10 % pump capacity and 823 s of stop time. This resulted in an inflow rate of 5 mL/h from 72 h of cultivation time until the end of the process. Samples were taken daily via the drain valve.

2.8. Determination of volumetric mass transfer coefficient with dynamic method

To determine the volumetric mass transfer coefficient (k_La) experimentally, the gas supply to the reactor was stopped at the end of the cultivation, the pO_2 value (dissolved oxygen concentration) was recorded for 5 min until the gas supply was turned back on and the pO_2 value was recorded again over time. The following formula, which takes OTR and oxygen uptake rate (OUR) into account, can be used for oxygen balancing [Garcia-Ochoa and Gomez, 2008; Moutafchieva et al., 2013]:

$$\frac{dc_{O_2}}{dt} = OTR - OUR, \text{ whereby}$$
$$OTR = k_L \cdot a \cdot (c^* - c_L) \quad (7)$$
$$\text{and } OUR = q_{O_2} \cdot X$$

Thereby, k_L is the mass transfer coefficient [ms^{-1}], a is the specific exchange surface area [m^{2}m^{-3}], c* is the saturation concentration of oxygen at the phase boundary [g/L], c_L the dissolved oxygen concentration in the core phase [g/L], q_{O2} the specific oxygen uptake rate [$\frac{g_{O2}}{g_{BTM} \cdot s}$ or $\frac{g}{L \cdot s}$] and X the biomass concentration [g/L]. By stopping the air supply, the value of the OTR becomes 0. Thus, with given biomass concentration, the OUR is determined from the slope of the plot of oxygen concentration against time. Thereby, the measured pO_2 values in % are converted to concentration values in g/L using the Henry coefficient of 0.0013 $\frac{mol}{L \cdot atm}$ for O_2 at standard conditions (water at 25 °C), a partial pressure of 0.2 atm and a molar weight of 32 g/mol, resulting in an oxygen concentration at 100 % saturation of $8.74 \cdot 10^{-3}$ g/L. After restarting the oxygen supply, stationary conditions are reached, so that $\frac{dc_{O_2}}{dt} = 0$ is valid and k_La is calculated by $\frac{OUR}{c^* - c_L}$.

2.9. Offline analytics

The biomass was determined as cell dry weight (BDW). In shake flasks cultivations the whole broth was filled in a pre-weighed 50 mL Falcon® tube and in stirred tank cultivations a 10 mL sample was filled in a pre-weighed 15 mL Falcon® tube and centrifuged for 10 min at 4° C and 4500 rpm (Hettich Rotixa 50 RS) or 9600 rpm (15 L NLF reactor samples; 6-16KS Sigma). The biomass pellet was dried in a drying oven at 100 °C for 48 h and weighed with an analytical balance (Ohaus PX 523). The supernatant was stored at –32 °C until carbon source, nitrogen and product concentration analysis. Nitrogen was quantified with Hang Lange cuvette test kits (LCK303 2–47 mg/L NH_4-N and LCK302 47–130 mg/L NH_4-N) in a spectrophotometer (Hach DR3900 VIS). The consumption of glucose and the production of 7dSh was monitored by measuring the samples, which were filtered (Rotilabo/Chrompure, cellulose acetate membrane, 0.2 µm, Carl Roth/Membrane Solutions) and 1:4 to 1:10 diluted, with an HPLC system (Knauer Azura, P 6.1 L pump,

AS 6.1 L Autosampler, Sykam S 41 20 Column oven, Sedere Sedex 85 ELSD-LT detector, carbohydrate lead column Biorad Aminex HPX-87P/ Agilent Technologies Hi-Plex Ca/ Macherey-Nagel VA 300 7.8 mm Nucleogel Sugar Pb, operated at 80 °C and a flow rate of 0.4 to 0.6 mL/ min with MilliQ water as eluent, injection volume of 15 to 40 µL). As standard for the determination of 7dSh concentration chemoenzymatic synthesized 7dSh as described by Brilisauer et al. [2019] was used in the beginning. Subsequently, 7dSh was purified from culture supernatants of *S. setonensis* cultivation (see 2.7) by extraction and chromatographic separation similar to the protocol described by Brilisauer et al. [2019], whereby the molecular identity was confirmed by NMR and concentration was determined via GC–MS [Braun, 2024].

3. Results and discussion

3.1. Design of experiments for identification of beneficial process conditions

To evolve a scalable, well-characterized bioprocess for an unknown microbial system, first, key factors (macro nutrients, osmolarity, filling volume and shaking speed) that influence growth of *S. setonensis* and benefit production of 7dSh were required to be examined (see 2.3). A DOE approach is a powerful tool that reduces the necessary number of experiments while still generating significant results and showing the influence of factors on each other and on the process [Mandenius and Brundin, 2008; Rosmine et al., 2017]. Therefore, a DOE batch approach in shake flasks was conducted (see 2.3) in minimal medium with varying concentrations of glucose (C source; 10 or 25 g/L), of ammonium sulphate (N source; 3 or 7.5 g/L) and of natrium chloride (0 or 11.7 g/L) (see 2.2). Thereby we chose the boundaries of the factors based on the hypothesis to enable growth but trigger stress responses or generate limiting conditions to increase 7dSh production (see 2.3).

The factorial regression model of the DOE revealed a significant effect of all five investigated factors on the 7dSh titer and one significant 2–way interaction of filling volume*shaking speed (forward selection of terms with $\alpha = 0.25$, resulting in the following regression equation in uncoded units 7dSh titer = 2.340 − 0.0337 vol + 3.614 Osm + 0.04057 C source − 0.0472 N source − 0.01272 speed + 0.000191 vol*speed; refer to Appendix Figure S8 for detailed statistical plots and model terms generated by the Minitab Software). The influence of each pair of factors on the 7dSh titer in g/L is displayed in contour plots in Fig. 1. Since the carbon source delivers energy and could serve as a precursor, its influence was anticipated and was not unexpected (high 7dSh titer zones in darker green for high glucose concentration, see Fig. 1, top row left to second from right). Although nitrogen is important for growth, it had a minor adverse effect on 7dSh production as the low titer zones are located at higher ammonium concentrations (in dark blue, see Fig. 1, top left and bottom center). Nevertheless, given that nitrogen is known to influence secondary metabolism, further investigation was conducted in the following experiments. The correlation between elevated osmolarity and a higher titer is clearly demonstrated by the high titer zones ranging from 0.15 to 0.2 M (in darker green, see Fig. 1, top right, second from right and bottom left). This might have several causes. Fuchino et al. [2017] demonstrated that a shift to higher osmolarity causes stronger branching at the lateral sites of *Streptomyces* hyphae, while most of the existing tips did not regrow. Furthermore, they showed that chromatin hypercondensation is a rapid response to an osmotic upshift, which may lead to differential gene expression [Fuchino et al., 2017]. In *S. coelicolor*, the production of the antibiotic undecylprodigiosin is enhanced at 2.5 % NaCl, whereas the production of actinorhodin is decreased. This is specific to higher osmolarity caused by salt, not by a non-ionic osmolyte, such as sucrose, and is likely to affect the expression of transcriptional activators of the pathway [Sevcikova and Kormanec, 2004], which might also be the case regarding 7dSh production. The expression of the stress response sigma factor σ^H is activated under salt stress and plays a role in differentiation [Kormanec et al., 2000; Sevcikova et al., 2001]. In response to salt stress, the intracellular concentration of proline rises [Killham and Firestone, 1984]. Proline acts as an osmo-protectant [Ameur et al., 2011], therefore the cells might be protected from damage caused by increased osmolarity. Changes in DNA supercoiling at high osmolarity [Cheung et al., 2003] lead to modulated effects of transcriptional regulators [Dorman, 1996] and might affect the 7dSh gene locus.

Hereafter, the two remaining parameters are considered, which

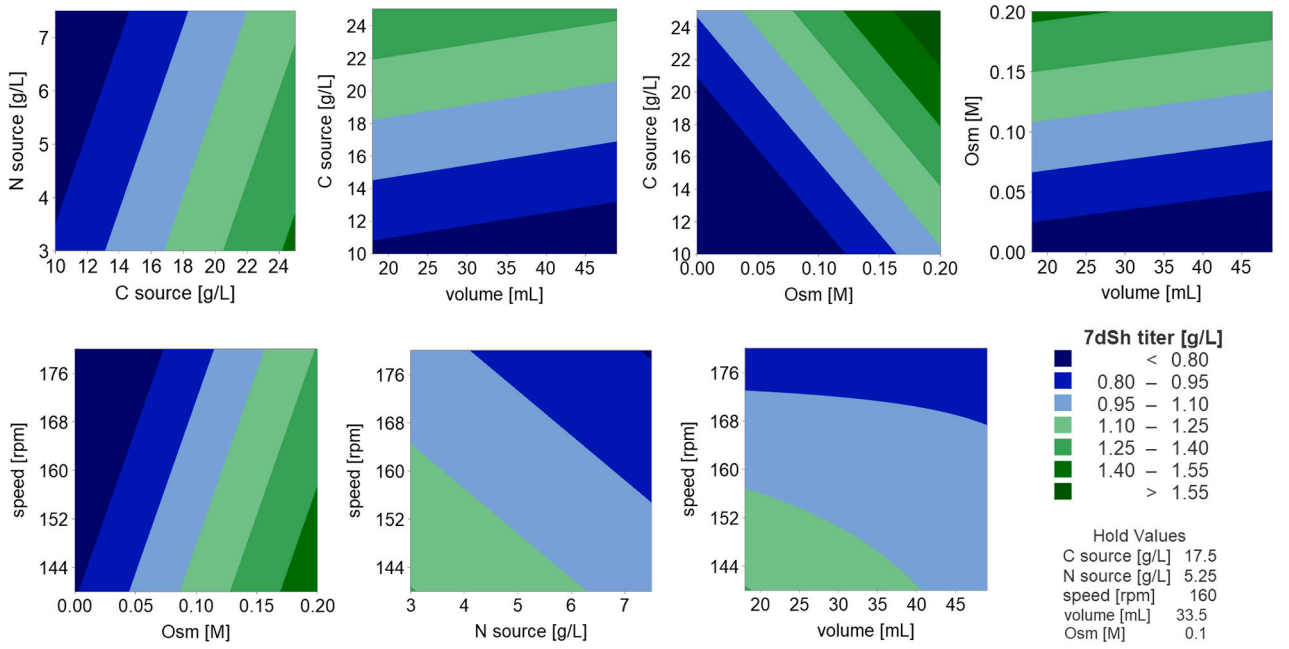

Fig. 1. Design of Experiments (DOE) for investigation of basic cultivation parameters in minimal medium, their significant influence on the 7dSh concentration and their reciprocal influence: A fractional factorial design (resolution III, linear model) was chosen with 5 factors at two levels (filling volume V_L 18 or 49 mL, shaking speed n 140 or 180 rpm, osmolarity (Osm) 0 or 0.2 M NaCl, C source concentration 10 or 25 g/L, N source concentration 3 or 7.5 g/L) and 7dSh titer as response, resulting in 8 boundary point experiments with three replicates (contour plots of 7dSh titer are displayed).

exerted a considerable effect on 7dSh titer (see Fig. 1). The advantage of lower shaking speed is less distinctive than the correlation of higher osmolarity with a higher 7dSh titer, as the high titer zones extend to 160 rpm for the dependence of shaking speed on both osmolarity and the nitrogen source (in green, see Fig. 1, bottom row). The relationship between shaking speed and filling volume illustrates an optimal shaking speed lower than 160 rpm with a beneficial filling volume of up to 40 mL (high 7dSh titer area in green, see Fig. 1, bottom right). However, when considering the dependency of filling volume on C source and on osmolarity, the advantage of lower shaking speed is less pronounced as the high titer area is less confined (green, Fig. 1, top right and second from left). This indicates that sufficient oxygen transfer was achieved by filling volumes of 18–40 mL while shaking at speeds lower than 160 rpm, thus avoiding the disadvantages of shear stress [Large et al., 1998; Mehmood et al., 2010; Omar et al., 2014]. This is consistent with the filamentous growth morphology as spherical pellets consisting of aggregated hyphal structures and investing resources for growth and production instead of cell repair and maintenance [Roubos et al., 2001; Zacchetti et al., 2018]. In conclusion, DOE limited the experimental effort and identified relevant factors, which were investigated further in subsequent experiments. The best combination of chosen parameters (25 g/L glucose, 3 g/L $(NH_4)_2SO_4$, 0.2 M NaCl, V_L = 18 mL, n = 140 rpm) resulted in a BDW of 5.2 ± 0.4 g/L and a 100–fold increase in 7dSh production, from 22 mg/L to 2.02 ± 0.26 g/L.

3.2. Investigation of process parameters in small scale

To verify the influence of oxygen availability on 7dSh production and gain a deeper understanding of the metabolism, the OTR was quantified with RAMOS® (see 2.4). Moreover, the effect of phosphate limitation and excess, which simultaneously influences the osmolarity, was examined in shake flasks and microtiter plates. Initially, it was investigated whether oxygen limitation occurs within the range of filling volumes applied during DOE cultivations (see 3.1). However, neither 30 mL, 40 mL nor 50 mL exhibited a characteristic OTR curve indicating oxygen limitation (see Appendix Figure S1). Oxygen transfer seems to have been fast enough in relation to the quite slow growth behavior, as the maximum OTR was reached within 220 h (see Appendix Figure S1). As phosphate concentration is known to influence metabolism and biosynthesis (see 2.4), the concentrations of the two phosphate components in the medium were varied by different factors and compared to the standard concentration (see 2.2). Thereby, Px1 stands for the standard concentration (with P representing the concentrations of the two phosphate components) and x1.5, x2 and x2.5 for the respective factors the phosphate concentrations were multiplied with. However, varying the phosphate concentration simultaneously affected the osmolarity of the medium, which was identified in the DOE experiment as a relevant factor (see 3.1). Therefore, the effect of a variation in the phosphate concentration was investigated with RAMOS® in minimal medium containing 20 g/L glucose in a batch process: on one hand with a varying NaCl concentration between 6.2 and 12 g/L to compensate for the elevated osmolarity caused by the elevated phosphate concentration (see Fig. 2A and 2B; see Appendix Table S3 for the calculation of ionic osmolarity) and on the other hand with a constant NaCl concentration (5.9 g/L) so that the osmolarity increased with the phosphate concentration (see Fig. 2B).

During cultivations involving an increase in phosphate and a decrease in NaCl concentration, the OTR exhibited a steep increase until 90 h after a lag phase of about 40 h (see Fig. 2A). Subsequently, the slope of the OTR decreased more markedly for the two lower phosphate concentrations (see Fig. 2A; OTR Px1 light blue, OTR Px1.5 turquoise). This may be due to inhibitory effects of decreasing pH values or of end- or by-products. The maximum OTR of 19 to 22 $\frac{mmol}{L \cdot h}$ was reached after 136 to 171 h. After 192 h glucose remained present at concentrations between 5.5 and 10.8 g/L. Although the C source has not been exhausted, the OTR decreased steeply for the lower phosphate concentrations (Px1, Px1.5) after OTR_{max} at 157 and 171 h. This indicates that another nutrient was limiting further metabolic activity. This beginning of cell decease was not observed at elevated phosphate concentrations (see Fig. 2A; OTR Px2 violet, OTR Px2.5 dark blue). Instead, the OTR entered a plateau phase, indicating a metabolic shift characterized by a higher product formation rate of 0.014 $\frac{g}{L \cdot h}$ compared to 0.003 $\frac{g}{L \cdot h}$ (Px1) and 0.006 $\frac{g}{L \cdot h}$ (Px1.5). The elevated phosphate levels also stabilized the pH value, in addition to the buffer. This resulted in a pH value of 6.7 for Px2.5 and 6.5 for Px2, compared to a pH value of 6.0 for Px1.5 and of 5.3 for Px1 at the end of the cultivation period, which may explain the prolonged life phase. Thereby the acidification of the culture medium when employing ammonium sulphate as N source is described also for another *Streptomyces* strain [Ren et al., 2014]. The biomass dry weight for all treatments lay within the same range, from 6.15 to 6.45 g/L with osmolarity compensation, and from 5.18 to 5.86 g/L for an equal initial

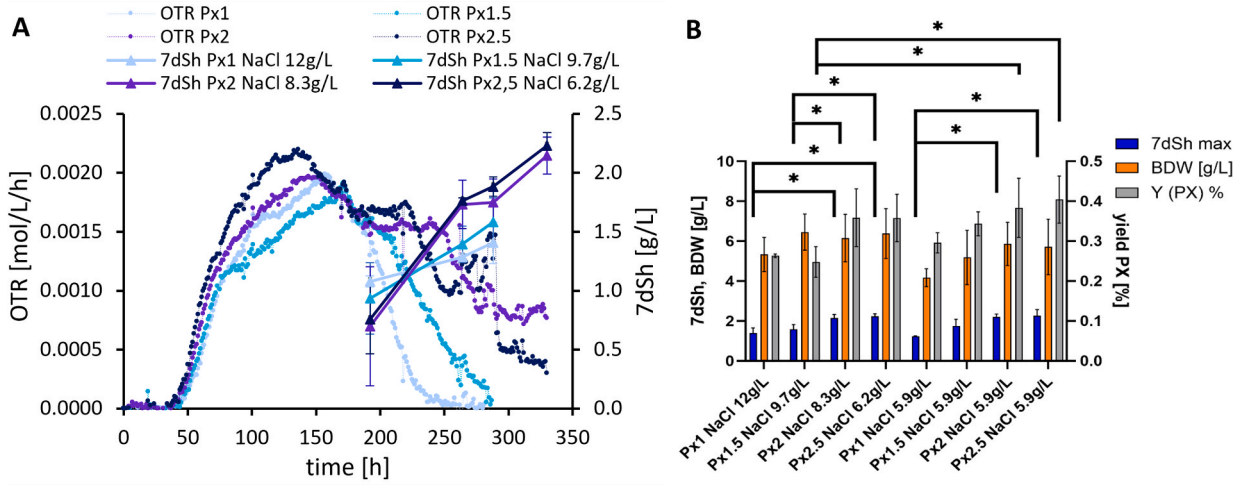

Fig. 2. Comparison of different amounts of the two phosphate components (change in concentration by factor 1 (Px1), 1.5 (Px1.5), 2 (Px2) and 2.5 (Px2.5)) of batch cultivation in minimal medium with 20 g/L glucose (250 mL flasks, 28 to 30 °C, 130 rpm, V_L = 33 mL, Inoculation 6 · 10^6 spores, standard P duplicate, elevated P quadruplicate): OTR measurement with RAMOS® and 7dSh concentration over time (**A**, compensation for increasing osmolarity by phosphate through decreasing NaCl concentration); Comparison of $7dSh_{max}$, biomass dry weight and product yield in relation to biomass Y_{PX} of varied phosphate concentrations with compensated osmolarity and without osmolarity compensation (**B**). Statistical analyses with ordinary one–way analysis of variance (ANOVA) for $7dSh_{max}$ and Y_{PX}, significant results indicated by * $p < 0.0332$, determined with Tukey's multiple comparisons test.

NaCl concentration, except for the lowest phosphate concentration with 5.33 and 4.17 g/L respectively (orange columns, Fig. 2B, differences are not significant (ns) with one–way ANOVA). This may have been caused by the lower pH value of this treatment as neutrophilic *Streptomyces* exhibit a pH optimum of 7 [Flowers and Williams 1978]. Growth and production of bioactive molecules at pH values of 5 or 6 depend heavily on the isolate in question [Bundale et al. 2015; Thakur et al. 2009]. When *S. setonensis* was cultivated at an initial pH value of 5, the average biomass dry weight after 10 days was only 0.56 g/L across eight treatments (data not shown). Another reason for lower biomass formation at Px1 may have been a lack of phosphate for ATP generation, which plays a fundamental role in cell growth and metabolite biosynthesis [Bonora et al., 2012; Mu et al., 2024]. The maximum produced 7dSh concentration with and without adjusted NaCl concentrations (blue columns, Fig. 2B) increased with the initial amount of phosphate (significant differences when comparing lower to higher phosphate concentrations). The product yield was higher for elevated phosphate concentrations (Px2, Px2.5), increasing with osmolarity (grey columns, Fig. 2B, ns except Px1.5 vs. Px2 and Px1.5 vs. Px2.5, one–way ANOVA). The higher 7dSh titer and yield for Px2 and Px2.5 can probably be attributed to a combination of effects. These include stabilized pH, which influences growth and biosynthesis, a higher amount of available phosphate for ATP generation and the beneficial effects of elevated osmolarity, as discussed previously (see 3.1).

Another RAMOS® experiment (see Appendix Figure S2) clearly demonstrated the growth retardation caused by elevated phosphate, when phosphate-limiting conditions (Px0.5) were compared to increasing phosphate concentrations at aligned osmolarity (Px1, Px2, Px3). Cultivation with limited phosphate showed a steep increase of OTR before the maximum, followed by a steep decrease (see Figure S2, curve in orange). Cultivations with higher amounts of phosphate exhibited a flatter OTR curve, indicating a lower growth rate but a prolonged growth phase (see Figure S2, curves in blue, yellow and grey). In conclusion, OTR measurements revealed that an elevated phosphate concentration may prolong the life span of the cells, first by decreasing the growth rate before reaching OTR_{max} compared to phosphate-limited conditions (Px0.5; see Appendix Figure S2) and, second, by decreasing the dying rate after reaching OTR_{max} (compared to Px1 and Px1.5; see Fig. 2A), which allowed for a prolonged stationary phase characterized by stable OTR values. During this stationary phase, the glucose concentration dropped to below 0.5 g/L, which explains the subsequent decline of OTR between 223 and 263 h (Px2.5) and 249 and 281 h (Px2), respectively (see OTR in violet and dark blue, Fig. 2A). Therefore, an option for prolonging this phase, during which the cells consume the carbon source and produce 7dSh, might be the application of a glucose feeding strategy. We hypothesized that this approach benefits 7dSh production, since the elevated 7dSh formation rate observed in phosphate-enriched media during the OTR plateau phase after OTR_{max} indicated that 7dSh formation is decoupled from growth.

In addition, different C sources (sucrose and starch) as well as reduced and increased trace element solution concentrations were investigated in preliminary experiments but did not result in improved 7dSh production. Furthermore, the influence of increasing phosphate concentrations, including limiting conditions (Px0.5), was investigated at two NaCl concentrations in a high-throughput microbioreactor (Biolector) for batch cultivation (see 2.5) in minimal medium with 25 g/L glucose (see 2.2). This involved increasing osmolarity by starting at one lower and one higher level of overall osmotic pressure and comparing this to an increasing osmolarity by adding NaCl at one phosphate concentration (see Fig. 3). The 7dSh titer increased significantly with increasing phosphate concentrations at lower osmolarity (0.1 M = 5.9 g/L NaCl; two–way ordinary ANOVA). At a higher osmolarity (0.2 M NaCl), the titer remained consistent across all phosphate concentrations (differences are ns). This result aligned with one RAMOS® experiment (see Appendix Figure S2), in which a variation of the phosphate concentration without influencing the osmolarity had no significant effect

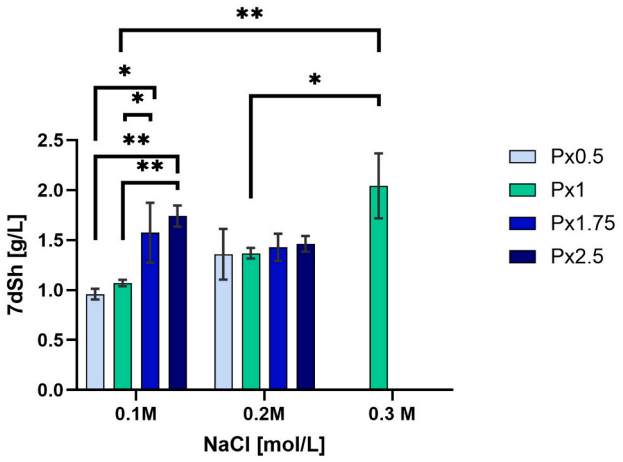

Fig. 3. Influence of an increasing phosphate concentration and osmolarity on produced 7dSh concentration in a batch cultivation in minimal medium with 25 g/L glucose in the Biolector (shaking speed 800 rpm, V_L = 1.2 mL, T = 30 °C): phosphate from limiting (Px0.5) over standard (Px1) to elevated concentration (Px1.75 and Px2.5) at two fixed NaCl concentrations (NaCl 0.1 M = 5.9 g/L; NaCl 0.2 M = 11.7 g/L). Comparison is made between an increasing osmolarity with increasing phosphate for two different starting levels of osmotic pressure and an increasing osmolarity by NaCl addition (0.1 M, 0.2 M, 0.3 M) at the standard phosphate concentration (Px1). Statistical analyses with ordinary two–way ANOVA (phosphate concentration and 0.1 M/ 0.2 M NaCl, n = 12) and one–way ANOVA (NaCl concentration variation at Px1, n = 9), only significant results of the Tukey's post–hoc analyses of the two aforementioned statistical comparisons are shown, indicated by * $p < 0.0332$ and ** $p < 0.0021$.

on the titer. Therefore, it seems that, once an osmolarity threshold has been reached, further increases in osmotic pressure due to phosphate had no additional beneficial effect on the 7dSh titer. A clear correlation is visible for the increase of the 7dSh titer with increasing osmolarity through the addition of NaCl at the standard phosphate concentration (see Fig. 3, green bars, Px1, ordinary one–way ANOVA).

In conclusion, the 7dSh titer increased with increasing osmolarity. Hence, higher phosphate is beneficial as it increases the osmolarity and causes changes in metabolism after the growth phase, thereby prolonging the stationary phase. These results provide a basis for investigating how cells can be maintained in this production phase for a longer period, thereby increasing the 7dSh titer. The next step was thus to develop a fed-batch process strategy.

3.3. Investigation of process mode in shake flasks

To avoid catabolite repression by glucose, we investigated a fed-batch operation regime (see 2.4), first at different phosphate concentrations (Px0.5, Px1, Px2.5) with an equal NaCl concentration. A higher 7dSh titer was reached during the fed-batch phase at the elevated phosphate concentration (Px2.5, see yellow curve in Appendix Figure S3). Thus, the feeding of the carbon source prolonged the production phase as assumed by previous results. Furthermore, the influence of constant glucose feeding compared to daily glucose pulses was investigated in another experiment (see Appendix Figure S4A) which clearly showed increasing OTR after glucose addition. However, no significant effect of constant feeding versus glucose pulses on 7dSh titer was detected by repeated measures two–way ANOVA. Batch experiments indicated non-growth-associated 7dSh production which is supported by the fed-batch results showing a pronounced increase in 7dSh concentration after OTR_{max} and the subsequent decline in OTR. Based on these findings, the following feeding experiment was performed in minimal medium with elevated phosphate concentration to improve constant feeding conditions and to investigate whether nitrogen is a limiting factor (see 2.4). After the first decrease in OTR was observed at

120 h (see Fig. 4), feeding with a 250 g/L glucose solution at a rate of 50 µL/h was employed until 190 h and again from 237 to 286 h. The OTR online monitoring data and the glucose and 7dSh concentrations over time are depicted in Fig. 4.

By constant glucose feeding, the OTR remained in the plateau phase that occurred after reaching OTR_{max}. A drop in OTR is prevented by providing the carbon source, which is displayed at 120 h for the replicate in lighter green (see Fig. 4A). This improved feeding operation raised the 7dSh titer to 4.5 ± 1.2 g/L which is the highest produced concentration reported so far (7dSh concentration shown in blue, Fig. 4A). For the cultivation with additional nitrogen supply there was a clearly visible increase in OTR during carbon source feeding from 120 h to 190 h and 237 h to 286 h and a decrease in OTR when feeding was stopped from 190 to 237 h (see Fig. 4B). In comparison, pulses of ammonia sulphate of 0.1 g at 67 h, 0.01 g at 215 h and 0.02 g at 237 h also caused an increase in OTR (displayed in grey, see Fig. 4B), but did not improve the overall 7dSh concentration (displayed in blue, Fig. 4B), which is in alignment with the DOE results (see 3.1). This aligns with the finding that nitrogen increases respiration [Martin and Demain, 1980] but stands in contrast to the demonstration of a positive effect on acarbose production of *Streptomyces* M37 by adding different ammonium salts (0.05 to 0.1 M) or Na–glutamate to the fermentation after 72 h of cultivation time [Ren et al. 2014]. It also contradicts reports of an antibiotic yield increase by supplementing nitrate while cultivating *S. lincolnensis* and *Amycolatopsis mediterranei* [Jin and Jiao, 1997; Shao et al., 2015]. On the other hand, a repeated-measures two–way ANOVA showed no significant difference of 7dSh titer of the two fed-batch processes with and without ammonium addition (blue dots, see Fig. 4A and Fig. 4B). Therefore, no repression effect of ammonium was detected on the 7dSh production as reported for the production of other secondary metabolites [Hobbs et al., 1992; Doull and Vining, 1990; Aharonowitz and Demain, 1979].

Furthermore, offline photometric nitrogen measurements confirmed that N source depletion correlates with the decrease in OTR at the end of the batch phase. This aligns with the results of Karandikar et al. [1997] for *S. coelicolor* A3(2) that the rapid growth phase ends when nitrate from the medium is depleted, but glucose consumption and low level biomass formation continues in the phase afterwards. During batch cultivation in elevated phosphate media, a biomass concentration of 5.7 ± 1.2 g/L was obtained (see Fig. 2A, Px2.5 media with 5.9 g/L NaCl), which is comparable to the biomass titer of 5.5 ± 0.3 g/L achieved in the fed-batch experiment using the same medium (see Fig. 4A).

In the fed-batch process, feeding was intentionally initiated after reaching OTR_{max} (between 91 h and 100 h), and the subsequent decline in OTR was taken as an indicator of the end of the growth phase. This strategy appeared to favor 7dSh formation, which in this study was predominantly observed after the growth phase. In the fed-batch process without additional nitrogen supply this was reflected by the marked increase in 7dSh concentration following OTR_{max}, so that the fed carbon enhanced 7dSh production without a further increase in biomass titer. In contrast, fed-batch cultivation with supplementary ammonium resulted in a substantially higher biomass concentration of 10.1 ± 2.4 g/L, which in turn led to a reduced product yield relative to biomass (Y_{PX}) from 0.82 g_{7dSh}/g_{BDW} to 0.33 g_{7dSh}/g_{BDW}. Accordingly, these results indicated that glucose feeding promotes biomass formation in the presence of sufficient nitrogen, while nitrogen limitation shifts carbon utilization toward 7dSh synthesis. Therefore, the feeding strategy evaluated in this study may be applicable to other bioprocesses involving secondary metabolite or non-growth-associated production.

The influence of extracellular nitrogen sources on secondary metabolite production in *Streptomyces* is governed by complex regulatory networks involving global response regulators and interactions with carbon and phosphate metabolism, which differs between species [Romero-Rodríguez et al. 2018; Tiffert et al., 2008]. In *S. venezuelae*, chloramphenicol production remained growth-coupled but was delayed in the presence of ammonium and temporarily inhibited by amino acids [Shapiro and Vining, 1983, 1984, 1985]. For *S. kanamyceticus* and *S. coelicolor,* production of kanamycin or actinorhodin is promoted by Na–nitrate, though prevented by different ammonium salts [Basak and Majumdar, 1973; Hobbs et al., 1990]. The utilization of nitrate increases the pH value of the cultivation medium and subsequently stabilizes it during the excretion of acidic by-products [Karandikar et al., 1997]. The consumption of glutamate as combined C and N source basifies the medium and after its depletion the production of actinorhodin begins [van Wezel et al., 2006]. Although N–acetylglucosamine has been demonstrated to stimulate antibiotic production in different *Streptomyces* species, this effect is not universal [Rigali et al., 2008]. In our experiments, no positive effect on 7dSh production was determined by feeding of nitrate with glucose or feed pulses of glutamate and N–acetyl-glucosamine (see Appendix Figure S4B). Moreover, the addition of ammonium or glutamate at different time points and growth on solely glutamate and/or N–acetyl-glucosamine did not yield any improvements of 7dSh production (data not shown). In conclusion, ammonium sulphate limited growth, its addition caused an increase in respiration and biomass formation but the 7dSh production in shake flasks was neither increased by adding the initial concentration of 3 g/L at the peak of the growth phase nor by adding low limiting concentrations of 5 mM (corresponding to 0.3 g/L) during the fed-batch phase (see Fig. 4B).

3.4. Scale-up to stirred tank reactor

Investigating scaling effects is essential for bioprocess development, as mixing, oxygen transfer, power input, spatial availability and pH control differ substantially when processes are transferred from small

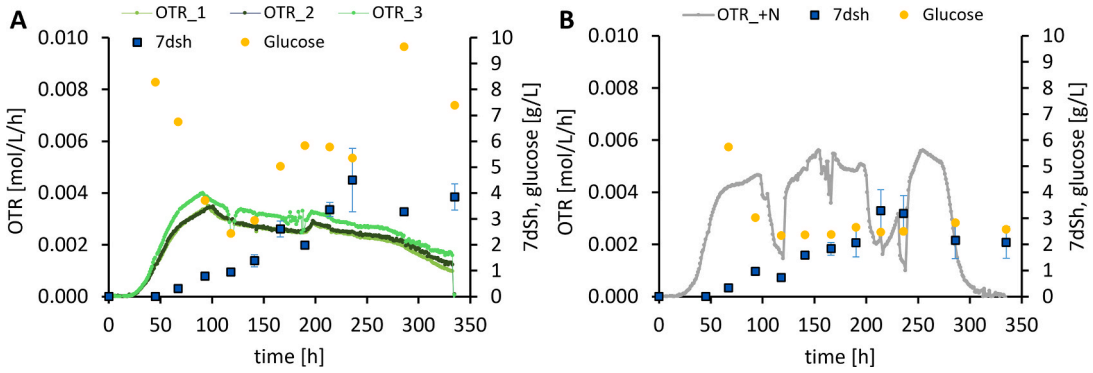

Fig. 4. Influence of improved constant feeding conditions on OTR, glucose and 7dSh concentration over time in minimal medium with 20 g/L glucose (250 mL flasks, 30 °C, 130 rpm, V_L = 33 mL, Inoculation 6 · 10^6 spores): constant feeding in elevated phosphate media (Px2.5) from 120 to 190 h and 237 to 286 h with 250 g/L glucose at a rate of 50 µL/h, pulse of 1 mL medium stock at 190 h and of 0.2 g NaCl at 216 h (**A**, triplicate), additional pulses of ammonium sulphate (**B**, duplicate) at 67 h 3 g/L, at 215 h 0.3 g/L, at 237 h 0.6 g/L and at 310 h 0.3 g/L.

scale in microtiter plates and shake flasks to larger scale in STRs. Since microbial processes often face oxygen limitations, k_La is frequently used as a scale-up criterion [Marques et al., 2010]. In order to increase k_La as well as OTR, the agitation rate can be increased which also alters the volumetric power input [Marques et al., 2010]. Under submerged cultivation conditions, *S. setonensis* exhibits a growth morphology in mycelial pellets. Therefore, our hypothesis, that the organism is susceptible to shear stress and thus lower agitation benefits 7dSh production, was confirmed by the DOE results (see 3.1). Moreover, we did not detect oxygen limitation under the applied process conditions in shake flasks (see 3.2 and Appendix Figure S1). Therefore, oxygen supply is not the primary limiting factor. We rather suspected that shear stress, which varied due to differing agitation methods across the applied cultivation systems during scale-up, represents a critical constraint. Consequently, we chose to keep the volumetric power input constant as a scaling strategy. This parameter was systematically calculated from the shake flasks to the 2 L stirred-tank reactor and subsequently to the 15 L stirred-tank reactor (see 2.6). We transferred the identified optimal conditions for a batch operation regime in shake flasks (see 3.1) to a 2 L twin bioreactor (see 2.7). The batch reactor cultivations with active pH control at 7 reached a 7dSh titer of 0.94 ± 0.07 g/L (see Appendix Figure S5A). We compared these cultivations to one reactor cultivation with osmolarity compensation for 0.1 M buffer reaching a comparable 7dSh titer of 1.05 g/L and one with MES buffer surprisingly reaching a 7dSh titer of 2.04 g/L (see Appendix Figure S5B and S5D). This was twice as much as for the other batch cultivations and resembled the titer in the shake flask cultivations (see Fig. 1 and 2). By employing repeated batch as process mode (see Appendix Figure S5C), the space–time-yield increased by factor 2.1 for the first repetition from 0.0079 ± 0.0006 $\frac{g}{L \cdot h}$ to 0.0168 ± 0.004 $\frac{g}{L \cdot h}$.

In shake flasks, the 7dSh titer doubled when we applied a fed-batch operation regime compared to the batch regime (compare Fig. 2A to Fig. 4A). In the course of this, medium with 2.5–fold higher phosphate concentration and 0.1 M NaCl was identified as a beneficial culture condition (see 3.3). Therefore, we investigated this process condition in a fed-batch cultivation in the 2 L STR in minimal media with 25 g/L glucose (see 2.7 and Fig. 5A). With a pump rate of 5.1 mL/h the glucose solution was fed in between 69 h and 127 h resulting in a rate of 0.3 $g_{glucose}$/h. A maximum 7dSh titer of 2.02 g/L was reached after 142 h of cultivation (see Fig. 5A), which was double the result of the batch fermentation. A comparable 7dSh titer was reached in the fed-batch cultivation performed in parallel with a standard phosphate concentration, 0.2 M NaCl for osmolarity compensation and a feeding rate of 0.6 $g_{glucose}$/h (see Appendix Figure S6A). Both treatments were repeated in parallel with another pre-culture, showing the same trend but with slightly lower maximum concentrations of biomass and 7dSh (see Appendix Figure S6B and S6C). At the lower glucose feed rate of 0.3 g/h (Fig. 5A), the glucose concentration steadily decreased from 11 to 2.5 g/L during the feeding period, in contrast to the higher feed rate of 0.6 g/h (Figure S6A) where the glucose concentration remained between 8 and 11.7 g/L from 79 h onwards until the end of the feeding period. For both treatments, the product formation rate between 47 and 142 h was 0.04 g/h, and the glucose consumption rate was 0.68 g/h for elevated phosphate medium (Fig. 5A) and 0.8 g/h for higher feed rate (Figure S6A). Interestingly, the biomass was in the same range with 9.6 g/L (Px2.5, 0.3 g/h feed) and 9.3 g/L (Px1, 0.6 g/h feed). Therefore, compared to elevated phosphate medium, the additional 17 g of glucose consumed at a higher feed rate, must be converted into another by-product. Therefore, elevated phosphate medium was chosen for further scale-up to a 15 L bioreactor, while considering the volumetric power input as the parameter to be kept constant (see 2.6). Feeding at a rate of 2.3 g/h was initiated at 72 h, with the glucose concentration remaining above 4 g/L until the end of the cultivation process at 242 h (see Fig. 5B). The resulting biomass of 7.6 g/L was slightly lower than in the 2 L bioreactor, as was the 7dSh concentration, which was 13.6 % lower than at smaller scale.

The oxygen volumetric mass transfer coefficient (k_La) of both reactor scales was determined experimentally with the dynamic method (see 2.8). Thereby, the slope of the regression line through the measurement points in the period without air supply yielded $1.032 \cdot 10^{-5} \frac{g}{L \cdot s}$ for the 2 L reactor (see Appendix Figure S7A), which is the specific oxygen uptake rate qo_2 of 7 g/L biomass, resulting in an OUR of $7.224 \cdot 10^{-5} \frac{g}{L \cdot s}$. With the reached stationary oxygen concentration c_L of 0.0049 g/L, $k_La = 0.019\ s^{-1}$. The OUR is equivalent to the OTR under stationary conditions. We thus compared it to the maximum OTR measured in shake flasks of $0.00483 \frac{mol}{L \cdot h} = 4.3 \cdot 10^{-5} \frac{g}{L \cdot s}$ (compare to Appendix Figure S3) and were able to show that the process conditions and calculated agitation speed by constant power input in the 2 L bioreactor enabled a higher OTR. For the 15 L bioreactor, qo_2 was determined with $8.71 \cdot 10^{-6} \frac{g}{L \cdot s}$ (see Appendix Figure S7B), resulting in an OUR of $6.367 \cdot 10^{-5} \frac{g}{L \cdot s}$ at a biomass concentration of 7.31 g/L. c_L was 0.0057 g/L, so that k_La yielded $0.021\ s^{-1}$. Although we calculated the scale-up agitation speed by maintaining a constant volumetric power input, the resulting volumetric mass transfer coefficient k_La was found to remain within a comparable range. This is often considered the more important parameter due to the

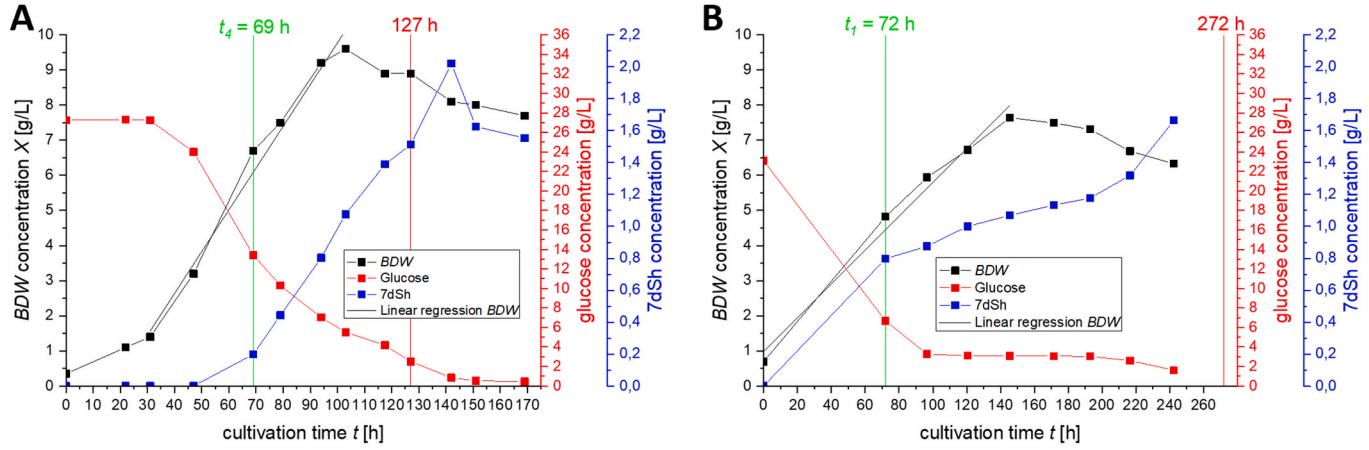

Fig. 5. Successful scale-up of fed-batch process to a 2 L bioreactor (**A**) and a 15 L bioreactor (**B**) in elevated phosphate minimal media (Px2.5, 0.1 M NaCl): biomass, glucose and 7dSh concentration over the cultivation time (**A**: one baffled 2 L STR with 2 Rushton turbines, 28 °C, V_L = 1.7 L, 5.1 mL/h feeding with 0.3 L of 61 g/L glucose solution from 69 h to 127 h, 250 rpm, aeration 1–2 vvm, addition of 0.2 – 0.3 mL antifoaming agent; **B**: one baffled STR with 3 Rushton turbines, 28 °C, V_L = 15 L, 5 mL/h feeding with 0.85 L of 465 g/L glucose solution from 72 h on, 290 rpm, aeration 1 vvm, overpressure of 0.2 bar, pH control at 7 with 2 M NaOH and 2 M phosphoric acid, automatic foam control, inoculation from 66 h batch in 2 L reactor).

common occurrence of oxygen limitations in aerobic bioprocesses which affect growth and production [Garcia-Ochoa and Gomez, 2008; de Souza et al., 2022]. In this context, our intention was to demonstrate that the approach of constant volumetric power input represents an equally valid scaling strategy, particularly for processes in which oxygen supply is not limiting, whereas sensitivity to shear stress constitutes a constraint. Such shear-related limitations have been reported for other *Streptomyces* species as well [Large et al. 1998; Zacchetti et al. 2018; Omar et al. 2014]. Since variations in agitation rate inherently influence the OTR, we additionally performed experimental k_La determinations, which independently supported the suitability of the selected scaling approach. Taken together, these results provide a rationale for not using k_La as the primary scale-up criterion in the present case, considering the specific morphology and growth characteristics of *S. setonensis*. Nevertheless, the maximal energy dissipation rate ε_{max} was 3.3 W/kg for the small scale and increased to 8.5 W/kg in the larger scale which might explain the slightly lower biomass and 7dSh formation in the 15 L bioreactor, which is still the highest titer reported in the larger scale so far. In conclusion, we successfully scaled up the process, laying the foundation for 7dSh production on a pilot-scale. Moreover, the process was developed to a stage at which sufficient quantities of this novel herbicide are available for subsequent purification and formulation experiments to investigate the use of 7dSh as granulate in sustainable agriculture.

As demonstrated by the comparison of batch and fed-batch cultivations in shake flasks, biomass formation was not increased in the fed-batch process in the absence of additional nitrogen supply (see 3.3). This observation was consistently confirmed at 2 L stirred-tank reactor scale, where comparable biomass concentrations were obtained in batch cultivation with pH control (9.55 ± 0.15 g/L) and in fed-batch cultivation (9.6 g/L). Since 7dSh production predominantly occurred after the growth phase, initiating the feed after the main biomass formation appears to promote the conversion of the supplied carbon into product rather than into additional cell mass.

Although downstream processing was beyond the scope of the present study, the natural occurring growth morphology as mycelial pellets of *S. setonensis* considerably simplifies biomass separation by sedimentation. This approach is analogous to other processes where cell agglomeration is induced, for example, by metal ion addition or co-cultivation of microalgae with filamentous fungi [Wang et al., 2021; Zhou et al., 2013]. Exploiting the inherent pellet formation is expected to significantly reduce downstream processing costs. While using defined media with glucose as the carbon source increases substrate costs, it simultaneously reduces overall processing costs compared to residual-stream-based processes, thereby supporting competitiveness with conventional products obtained from fossil raw materials [Jain and Kumar, 2024]. Crude fermentation broth, from which only the cells had been removed, was applied to solid growth media plates as a herbicide and demonstrated effectiveness against plant seedlings in preliminary experiments (refer to Appendix Figure S9). These results therefore indicate the feasibility of a simple and low-cost downstream strategy, which should be further investigated in future studies.

Furthermore, the next stage in process development is the integration of agricultural or food-processing waste streams, such as hydrolyzed sugar beet pulp rich in readily fermentable sugars [Usmani et al., 2021], into the fermentation process. This step builds on the process understanding established in the present study and will allow the evaluation of such substrates with respect to process robustness and economic viability, thereby contributing to the development of a more sustainable process and supporting concepts of circular economy and biorefinery.

4. Conclusion

In conclusion, this study demonstrates the systematic development of a well-characterized and scalable bioprocess with *Streptomyces setonensis* to produce 7dSh. The extended stationary phase due to increased phosphate concentrations enabled the implementation of an effective feeding strategy, which improved the 7dSh titer by a factor of 200, from 22 mg/L to over 4 g/L. Although k_La is frequently applied as a scale-up criterion, the present study demonstrates that calculating the volumetric power input is a suitable alternative for shear-stress sensitive, pellet-forming organisms, particularly under oxygen-unlimited conditions. This strategy enabled a successful scale-up from shake flasks to a 15 L stirred-tank reactor, providing a solid foundation for pilot-scale production. Future work should leverage the gained process understanding to integrate agro-industrial waste streams as alternative substrates and to evaluate downstream options that exploit the simple sedimentation-based separation of cell pellets from the 7dSh containing broth. Overall, the achieved titer highlights the potential of microbial 7dSh production for providing a bio-based herbicide, competitive to conventional chemical products.

Declaration of generative AI and AI-assisted technologies in the writing process

Statement: During the preparation of this work the authors used DeepL Write in order to improve the readability of the text. The authors reviewed and edited the text as needed and take full responsibility for the content of the published article.

CRediT authorship contribution statement

X. Steurer: Writing – review & editing, Writing – original draft, Visualization, Validation, Methodology, Investigation, Formal analysis, Data curation, Conceptualization. **B. Kalik:** Visualization, Investigation, Formal analysis. **D. Jakobs-Schönwandt:** Writing – review & editing, Validation, Project administration, Funding acquisition. **A. Grünberger:** Writing – review & editing, Supervision, Conceptualization. **A. V. Patel:** Validation, Resources, Project administration, Funding acquisition.

Funding

This work was supported by the German Federal Ministry of Education and Research (BMBF) and VDI/VDE Innovation + Technik GmbH under the project grant 03VP09362 7dSherbizid. Open access publication was funded by Hochschule Bielefeld – University of Applied Sciences and Arts (HSBI).

Declaration of competing interest

The authors declare that they have no known competing financial interests or personal relationships that could have appeared to influence the work reported in this paper.

Acknowledgements

We greatly acknowledge Dr. Risse, working group Multiscale Bioengineering and Center for Biotechnology, Faculty of Technology, University Bielefeld for providing technical support and the access to the 19L NLF Bioengineering reactor for scale-up as well as Prof. Dr. Forchhammer, department of Microbiology and Organismic Interactions, University of Tübingen and the Research Laboratories, MeGi Seika Kaisha Ltd., Morooka, Yokohama, Japan for providing the microbial strain used in this study. We sincerely thank Dr. Marvin Braun, ZMBP, University of Tübingen for GC-MS measurements and effect testing on plant seedlings, as well as Nathan von Manteuffel, University of Tübingen for downstream processing experiments. Moreover, we would like to express our gratitude to Dr. Muth, department of Microbial Bioactive Compounds, University of Tübingen for advice regarding the handling of Streptomyces, to Ms. Blanck, University of Applied Sciences and Arts (HSBI), for English editorial, to Mr. Nelles and Dr. Trutnau, HiTec Zang GmbH for technical support with the RAMOS® device and to

Mr. Meyer and Mr. Dahlheim, Beckman Coulter GmbH for BioLector technical support.

Appendix A. Supplementary data

Supplementary data to this article can be found online at https://doi.org/10.1016/j.biortech.2026.134217.

Data availability

Data will be made available on request.

References

Aharonowitz, Y., Demain, A.L., 1979. Nitrogen nutrition and regulation of cephalosporin production in *Streptomyces clavuligerus*. Can. J. Microbiol. 25 (1), 61–67. https://doi.org/10.1139/m79-010.

Ameur, H., Ghoul, M., Selvin, J., (2011). The osmoprotective effect of some organic solutes on Streptomyces sp. mado2 and nocardiopsis sp. mado3 growth. Braz J Microbiol. 1;42(2):543–553. Doi: 10.1590/s1517-838220110002000019.

Anderlei, T., Büchs, J., (2001). Device for sterile online measurement of the oxygen transfer rate in shaking flasks. Biochem Eng J. Mar,7(2), 157–162. Doi: 10.1016/s1369-703x(00)00116-9.

Anderlei, T., Zang, W., Papaspyrou, M., Büchs, J., 2004. Online respiration activity measurement (OTR, CTR, RQ) in shake flasks. Biochem. Eng. J. 17, 187–194. https://doi.org/10.1016/s1369-703x(03)00181-5.

Barka, E.A., Vatsa, P., Sanchez, L., Gaveau-Vaillant, N., Jacquard, C., Klenk, H.-P., Clément, C., Ouhdouch, Y., Van Wezel, G.P., 2016. Taxonomy, physiology, and natural products of actinobacteria. Microbiol Mol Biol Rev 80, 1–43. https://doi.org/10.1128/mmbr.00019-15.

Basak, K., Majumdar, S.K., 1973. Utilization of carbon and nitrogen sources by streptomyces kanamyceticus for kanamycin production. Antimicrob. Agents Chemother. 4, 6–10. https://doi.org/10.1128/aac.4.1.6.

Bates, R.L., Fondy, P.L., Corpstein, R.R., 1963. Examination of some geometric parameters of impeller power. Ind. Eng. Chem. Process Des. Dev. 2 (4), 310–314. https://doi.org/10.1021/i260008a011.

Battaglin, W.A., Meyer, M.T., Kuivila, K.M., Dietze, J.E., 2014. Glyphosate and its degradation product AMPA occur frequently and widely in U.S. soils, surface water, groundwater, and precipitation. JAWRA J. Am. Water Resour. Assoc. 50, 275–290. https://doi.org/10.1111/jawr.12159.

Bonora, M., Patergnani, S., Rimessi, A., De Marchi, E., Suski, J.M., Bononi, A., Giorgi, C., Marchi, S., Missiroli, S., Poletti, F., Wieckowski, M.R., Pinton, P., 2012. ATP synthesis and storage. Purinergic Signalling 8, 343–357. https://doi.org/10.1007/s11302-012-9305-8.

Braun, M., (2024). 7dSh as New Sustainable Herbicide: Unravelling Physiological Responses and Action Mechanisms. Ph.D. Thesis (Thesis advisor Harter, K.), Eberhard Karls University Tübingen, Germany. Publication server of Tuebingen University, 7 Faculty of Mathematics and Natural Sciences. https://doi.org/10.15496/publikation-101001.

Brilisauer, K., Rapp, J., Rath, P., Schöllhorn, A., Bleul, L., Weiss, E., Stahl, M., Grond, S., Forchhammer, K., 2019. Cyanobacterial antimetabolite 7-deoxy-sedoheptulose blocks the shikimate pathway to inhibit the growth of prototrophic organisms. Nat. Commun. 10, 545.

Büchs, J., Maier, U., Milbradt, C. Zoels, B., (2000). Power consumption in shaking flasks on rotary shaking machines: I. Power consumption measurement in unbaffled flasks at low liquid viscosity. Biotechnol. Bioeng., 68, 6, pp. 589-593, Doi: 10.1002/(SICI)1097-0290(20000620)68:6****589::AID-BIT1***3.0.CO;2-J.

Bundale, S., Begde, D., Nashikkar, N., Kadam, T., Upadhyay, A., 2015. Optimization of culture conditions for production of bioactive metabolites by streptomyces spp. isolated from soil. Adv. Microbiol. 5, 441–451. https://doi.org/10.4236/aim.2015.56045.

Busi, R., Vila-Aiub, M.M., Beckie, H.J., Gaines, T.A., Goggin, D.E., Kaundun, S.S., Lacoste, M., Neve, P., Nissen, S.J., Norsworthy, J.K., Renton, M., Shaner, D.L., Tranel, P.J., Wright, T., Yu, Q., Powles, S.B., 2013. Herbicide-resistant weeds: from research and knowledge to future needs. Evol. Appl. 6, 1218–1221. https://doi.org/10.1111/eva.12098.

Carroll, A.L., Case, A.E., Zhang, A., Atsumi, S., 2018. Metabolic engineering tools in model cyanobacteria. Metab. Eng. 50, 47–56. https://doi.org/10.1016/j.ymben.2018.03.014.

Cheung, K.J., Badarinarayana, V., Selinger, D.W., Janse, D., Church, G.M., 2003. A microarray-based antibiotic screen identifies a regulatory role for supercoiling in the osmotic stress response of *Escherichia coli*. Genome Res. 13 (2), 206–215. https://doi.org/10.1101/gr.401003.

Cui, Y.Q., Van der Lans, R.G.J.M., Luyben, K.C.A.M., 1996. Local power uptake in gas-liquid systems with single and multiple rushton turbines. Chem. Eng. Sci. 51, 2631–2636. https://doi.org/10.1016/0009-2509(96)00128-5.

Davy, A.M., Kildegaard, H.F., Andersen, M.R., 2017. Cell factory engineering. Cell Syst. 4, 262–275. https://doi.org/10.1016/j.cels.2017.02.010.

Desai, S., Kumar, G.P., Amalraj, E.L.D., Talluri, V.R., Peter, A.J., 2016. Challenges in regulation and registration of biopesticides: an overview. In: Singh, D., Singh, H., Prabha, R. (Eds.), Microbial Inoculants in Sustainable Agricultural Productivity. Springer, New Delhi. https://doi.org/10.1007/978-81-322-2644-4_19.

Dorman, C., 1996. Flexible response: DNA supercoiling, transcription and bacterial adaptation to environmental stress. Trends Microbiol. 4 (6), 214–216. https://doi.org/10.1016/0966-842x(96)30015-2.

Doull, J.L., Vining, L.C., 1990. Nutritional control of actinorhodin production by *Streptomyces coelicolor* A3(2): suppressive effects of nitrogen and phosphate. Appl. Microbiol. Biotechnol. 32, 449–454. https://doi.org/10.1007/BF00903781.

Duke, S.O., Powles, S.B., 2008. Glyphosate: a once-in-a-century herbicide. Pest Manag. Sci. 64, 319–325. https://doi.org/10.1002/ps.1518.

Duke, S.O., Powles, S.B., 2009. Glyphosate-resistant crops and weeds: now and in the future. AgBioforum 12, 346–357.

Duke, S.O., Stidham, M.A., Dayan, F.E., 2018. A novel genomic approach to herbicide and herbicide mode of action discovery. Pest Manag. Sci. 75, 314–317. https://doi.org/10.1002/ps.5228.

Dzhavakhiya, V., Savushkin, V., Ovchinnikov, A., Glagolev, V., Savelyeva, V., Popova, E., Novak, N., Glagoleva, E., (2016). Scaling up a virginiamycin production by a high-yield *Streptomyces virginiae* VKM Ac-2738D strain using adsorbing resin addition and fed-batch fermentation under controlled conditions. 3 Biotech, 6(2):240. Doi: 10.1007/s13205-016-0566-8.

Elsayed, E.A., Omar, H.G., El-Enshasy, H.A., 2015. Development of fed-batch cultivation strategy for efficient oxytetracycline production by streptomyces rimosus at semi-industrial scale. Braz. Arch. Biol. Technol. 58, 676–685. https://doi.org/10.1590/s1516-89132015050184.

Ezaki, N., Tsuruoka, T., Ito, T., Niida, T., 1970. Studies on new antibiotics, SF-666 a and B. I. isolation and characterization of SF-666 a and B. Sci. Rept Meiji Seika Kaisha 11, 15–20.

Farina, W.M., Balbuena, M.S., Herbert, L.T., Mengoni Goñalons, C., Vázquez, D.E., 2019. Effects of the herbicide glyphosate on honey bee sensory and cognitive abilities: individual impairments with implications for the hive. Insects 10 (10), 354. https://doi.org/10.3390/insects10100354.

Ferraiuolo, S.B., Cammarota, M., Schiraldi, C., Restaino, O.F., 2021. Streptomycetes as platform for biotechnological production processes of drugs. Appl. Microbiol. Biotechnol. 105, 551–568. https://doi.org/10.1007/s00253-020-11064-2.

Flowers, T.H., Williams, S.T., 1978. The influence of pH on the growth rate and viability of neutrophilic and acidophilic streptomycetes. Microbios 18 (73–74), 223–228. PMID: 27702.

Fuchino, K., Flärdh, K., Dyson, P., Ausmees, N., 2017. Cell-biological studies of osmotic shock response in Streptomyces spp. J. Bacteriol. 199, e00465–e00516. https://doi.org/10.1128/JB.00465-16.

Gallagher, K.A., Wanger, G., Henderson, J., Llorente, M., Hughes, C.C., Jensen, P.R., 2017. Ecological implications of hypoxia-triggered shifts in secondary metabolism. Environ. Microbiol. 19 (6), 2182–2191. https://doi.org/10.1111/1462-2920.13700.

Gamboa-Suasnavart, R.A., Valdez-Cruz, N.A., Gaytan-Ortega, G., Reynoso-Cereceda, G.I., Cabrera-Santos, D., López-Griego, L., Klöckner, W., Büchs, J., Trujillo-Roldán, M.A., 2018. The metabolic switch can be activated in a recombinant strain of Streptomyces lividans by a low oxygen transfer rate in shake flasks. Microb. Cell Fact. 17, 189. https://doi.org/10.1186/s12934-018-1035-3.

Gandhi, K., Khan, S., Patrikar, M., Markad, A., Kumar, N., Choudhari, A., Sagar, P., Indurkar, S., 2021. Exposure risk and environmental impacts of glyphosate: highlights on the toxicity of herbicide co-formulants. Environ. Challenges 4, 100149. https://doi.org/10.1016/j.envc.2021.100149.

Gandini, E.M.M., Costa, E.S.P., Santos, J.B.D., Soares, M.A., Barroso, G.M., Corrêa, J.M., Carvalho, A.G., Zanuncio, J.C., 2020. Compatibility of pesticides and/or fertilizers in tank mixtures. J. Clean. Prod. 268, 122152. https://doi.org/10.1016/j.jclepro.2020.122152.

Garcia-Ochoa, F., Gomez, E., 2008. Bioreactor scale-up and oxygen transfer rate in microbial processes: an overview. Biotechnol. Adv. 27, 153–176. https://doi.org/10.1016/j.biotechadv.2008.10.006.

Giese, H., Klöckner, W., Peña, C., Galindo, E., Lotter, S., Wetzel, K., Meissner, L., Peter, C. P., Büchs, J., 2014. Effective shear rates in shake flasks. Chem. Eng. Sci. 118, 102–113. https://doi.org/10.1016/j.ces.2014.07.037.

Gómez-Ríos, D., Junne, S., Neubauer, P., Ochoa, S., Ríos-Estepa, R., Ramírez-Malule, H., 2019. Characterization of the metabolic response of streptomyces clavuligerus to shear stress in stirred tanks and single-use 2D rocking motion bioreactors for clavulanic acid production. Antibiotics 8, 168. https://doi.org/10.3390/antibiotics8040168.

Gómez-Ríos, D., Ramírez-Malule, H., Neubauer, P., Junne, S., Ríos-Estepa, R., Ochoa, S., 2022. Tuning of fed-batch cultivation of *Streptomyces clavuligerus* for enhanced Clavulanic Acid production based on genome-scale dynamic modeling. Biochem. Eng. J. 185, 108534. https://doi.org/10.1016/j.bej.2022.108534.

Guan, A., He, Z., Wang, X., Jia, Z.-J., Qin, J., 2024. Engineering the next-generation synthetic cell factory driven by protein engineering. Biotechnol. Adv. 73, 108366. https://doi.org/10.1016/j.biotechadv.2024.108366.

Guez, J.S., Müller, C.H., Danze, P.M., Büchs, J., Jacques, P., 2008. Respiration activity monitoring system (RAMOS), an efficient tool to study the influence of the oxygen transfer rate on the synthesis of lipopeptide by *Bacillus subtilis* ATCC6633. J. Biotechnol. 134, 121–126. https://doi.org/10.1016/j.jbiotec.2008.01.003.

He, B., Hu, Y., Wang, W., Yan, W., Ye, Y., 2022. The progress towards novel herbicide modes of action and targeted herbicide development. Agronomy 12, 2792. https://doi.org/10.3390/agronomy12112792.

Hobbs, G., Frazer, C.M., Gardner, D.C.J., Cullum, J.A., Oliver, S.G., 1989. Dispersed growth of Streptomyces in liquid culture. Appl. Microbiol. Biotechnol. 31, 272–277. https://doi.org/10.1007/BF00258408.

Hobbs, G., Frazer, C.M., Gardner, D.C.J., Flett, F., Oliver, S.G., 1990. Pigmented antibiotic production by *Streptomyces coelicolor* A3(2): kinetics and the influence of nutrients. J. Gen. Microbiol. 136, 2291–2296. https://doi.org/10.1099/00221287-136-11-2291.

Hobbs, G., Obanye, A.I., Petty, J., Mason, J.C., Barratt, E., Gardner, D.C., Flett, F., Smith, C.P., Broda, P., Oliver, S.G., 1992. An integrated approach to studying regulation of production of the antibiotic methylenomycin by *Streptomyces coelicolor* A3(2). J. Bacteriol. 174, 1487–1494. https://doi.org/10.1128/jb.174.5.1487-1494.1992.

Hopwood DA. 2007. Streptomyces in nature and medicine: the antibiotic makers. Oxford University Press, New York, NY. Doi: 10.1093/oso/9780195150667.001.0001.

Hudcova, V., Machon, V., Nienow, A.W., 1989. Gas–liquid dispersion with dual Rushton impellers. Biotechnol. Bioeng. 34, 617–628. https://doi.org/10.1002/bit.260340506.

Jain, S., Kumar, S., 2024. A comprehensive review of bioethanol production from diverse feedstocks: current advancements and economic perspectives. Energy 296, 131130. https://doi.org/10.1016/j.energy.2024.131130.

Jin, Z., Jiao, R., 1997. Stimulative effects of nitrate and magnesium salts on biosynthesis of lincomycin by Streptomyces lincolnensis. Sheng Wu Hua Xue Za Zhi = Chin. Biochem. J. 13 (6), 709–715.

Kaiser, S.C., Werner, S., Jossen, V., Blaschczok, K., Eibl, D., 2018. Power input measurements in stirred bioreactors at laboratory scale. J. Vis. Exp. 135, e56078. https://doi.org/10.3791/56078.

Kanno, M., Carroll, A.L., Atsumi, S., 2017. Global metabolic rewiring for improved CO2 fixation and chemical production in cyanobacteria. Nat. Commun. 8. https://doi.org/10.1038/ncomms14724.

Karandikar, A., Sharples, G.P., Hobbs, G., 1997. Differentiation of *Streptomyces coelicolor* A3(2) under nitrate-limited conditions. Microbiology 143 (11), 3581–3590. https://doi.org/10.1099/00221287-143-11-3581.

Kiefer, J.S.T., Batsukh, S., Bauer, E., Hirota, B., Weiss, B., Wierz, J.C., Fukatsu, T., Kaltenpoth, M., Engl, T., 2021. Inhibition of a nutritional endosymbiont by glyphosate abolishes mutualistic benefit on cuticle synthesis in Oryzaephilus surinamensis. Commun. Biol. 4, 554. https://doi.org/10.1038/s42003-021-02057-6.

Killham, K., Firestone, M.K., 1984. Proline transport increases growth efficiency in salt-stressed *Streptomyces griseus*. Appl. Environ. Microbiol. 48 (1), 239–241. https://doi.org/10.1128/aem.48.1.239-241.1984.

Klátyik, S., Simon, G., Oláh, M., Takács, E., Mesnage, R., Antoniou, M.N., Zaller, J.G., Székács, A., 2024. Aquatic ecotoxicity of glyphosate, its formulations, and co-formulants: evidence from 2010 to 2023. Environ. Sci. Eur. 36, 22. https://doi.org/10.1186/s12302-024-00849-1.

Knezevic, S.Z., Jhala, A., Gaines, T., (2016). Herbicide Resistance and Molecular Aspects, in: Elsevier eBooks. S. 455–458. Doi: 10.1016/b978-0-12-394807-6.00025-3.

Koepff, J., Sachs, C.C., Wiechert, W., Kohlheyer, D., Noeh, K., Oldiges, M., Grünberger, A., 2018. Germination and growth analysis of streptomyces lividans at the single-cell level under varying medium compositions. Front. Microbiol. 9, 2680. https://doi.org/10.3389/fmicb.2018.02680.

Kominek, L.A., 1972. Biosynthesis of novobiocin by *Streptomyces niveus*. Antimicrob Agents Chemotherapy 1 (2), 123–134. https://doi.org/10.1128/AAC.1.2.123.

Kormanec, J., Sevcikova, B., Halgasova, N., Knirschova, R., Rezuchova, B., 2000. Identification and transcriptional characterization of the gene encoding the stress-response sigma factor σ^H in *Streptomyces coelicolor* A3(2). FEMS Microbiol. Lett. 189, 31–38. https://doi.org/10.1111/j.1574-6968.2000.tb09202.x.

Kracík, T., Moucha, T., 2021. Ungassed power input prediction in stirred tank reactors. Chem. Pap. 76, 293–300. https://doi.org/10.1007/s11696-021-01854-x.

Lai, M.J., Tsai, J.C., Lan, E.I., 2022. CRISPRi-enhanced direct photosynthetic conversion of carbon dioxide to succinic acid by metabolically engineered cyanobacteria. Bioresour. Technol. 366, 128131. https://doi.org/10.1016/j.biortech.2022.128131.

Large, K.P., Ison, A.P., Williams, D.J., 1998. The effect of agitation rate on lipid utilisation and clavulanic acid production in *Streptomyces clavuligerus*. J. Biotechnol. 63 (2), 111–119. https://doi.org/10.1016/s0168-1656(98)00082-0.

LeBaron, H.M., Hill, E.R., (2008). Weeds resistant to nontriazine classes of herbicides. In: LeBaron HM, McFarland JE, Burnside OC (eds) The Triazine Herbicides. Elsevier, Chapter 11. Doi: 10.1016/B978-0-444-51167-6.X5001-6.

Liu, G., Chater, K.F., Chandra, G., Niu, G., Tan, H., 2013. Molecular regulation of antibiotic biosynthesis in streptomyces. Microbiol Mol Biol Rev 77, 112–143. https://doi.org/10.1128/mmbr.00054-12.

Liu, X., Xie, H., Roussou, S., Lindblad, P., 2022. Current advances in engineering cyanobacteria and their applications for photosynthetic butanol production. Curr. Opin. Biotechnol. 73, 143–150. https://doi.org/10.1016/j.copbio.2021.07.014.

López-García, M.T., Rioseras, B., Yagüe, P., Álvarez, J.R., Manteca, Á., 2014. Cell immobilization of *Streptomyces coelicolor* : effect on differentiation and actinorhodin production. Int. Microbiol. 17, 75–80. https://doi.org/10.2436/20.1501.01.209.

Lovell, S.T., Wax, L.M., Horak, M.J., Peterson, D.E., 1996. Imidazolinone and sulfonylurea resistance in a biotype of common waterhemp (amaranthus rudis). Weed Sci. 44, 789–794. https://doi.org/10.1017/s0043174500094728.

Maier, U., Büchs, J., 2001. Characterisation of the gas–liquid mass transfer in shaking bioreactors. Biochem. Eng. J. 7, 99–106. https://doi.org/10.1016/s1369-703x(00)00107-8.

Mandenius, C., Brundin, A., 2008. Bioprocess optimization using design-of-experiments methodology. Biotechnol. Prog. 24 (6), 1191–1203. https://doi.org/10.1002/btpr.67.

Marques, M.P.C., Cabral, J.M.S., Fernandes, P., 2010. Bioprocess scale-up: quest for the parameters to be used as criterion to move from microreactors to lab-scale. J. Chem. Technol. Biotechnol. 85, 1184–1198. https://doi.org/10.1002/jctb.2387.

Martin, J.F., 2004. Phosphate control of the biosynthesis of antibiotics and other secondary metabolites is mediated by the PhoR-PhoP system: an unfinished story. J. Bacteriol. 186 (16), 5197–5201.

Martin, J.F., Demain, A.L., 1980. Control of antibiotic biosynthesis. Microbiol. Rev. 44, 230–251. https://doi.org/10.1128/mr.44.2.230-251.1980.

Martin, J.F., McDaniel, L.E., 1975. Kinetics of biosynthesis of polyene macrolide antibiotics in batch cultures: cell maturation time. Biotechnol. Bioeng. 17, 925–938. https://doi.org/10.1002/bit.260170611.

Meftaul, I.M., Venkateswarlu, K., Dharmarajan, R., Annamalai, P., Asaduzzaman, M., Parven, A., Megharaj, M., 2020. Controversies over human health and ecological impacts of glyphosate: is it to be banned in modern agriculture? Environ. Pollut. 263 (Pt A), 114372. https://doi.org/10.1016/j.envpol.2020.114372.

Mehmood, N., Olmos, E., Marchal, P., Goergen, J., Delaunay, S., 2010. Relation between pristinamycins production by Streptomyces pristinaespiralis, power dissipation and volumetric gas–liquid mass transfer coefficient, kLa. Process Biochem. 45, 1779–1786. https://doi.org/10.1016/j.procbio.2010.02.023.

Meier, K., Klöckner, W., Bonhage, B., Antonov, E., Regestein, L., Büchs, J., 2016. Correlation for the maximum oxygen transfer capacity in shake flasks for a wide range of operating conditions and for different culture media. Biochem. Eng. J. 109, 228–235. https://doi.org/10.1016/j.bej.2016.01.014.

Mohd Ghazi, R., Nik Yusoff, N.R., Abdul Halim, N.S., Wahab, I.R.A., Ab Latif, N., Hasmoni, S.H., Zaini, M.A.A., Zakaria, Z.A., 2023. Health effects of herbicides and its current removal strategies. Bioengineered 14 (1). https://doi.org/10.1080/21655979.2023.2259526.

Montesinos, E., 2003. Development, registration and commercialization of microbial pesticides for plant protection. Int. Microbiol. 6, 245–252. https://doi.org/10.1007/s10123-003-0144-x.

Moutafchieva, D., Popova, D., Dimitrova, S., Tchaoushev, S., 2013. Experimental determination of the volumetric mass transfer coefficient. J. Chem. Technol. Metal 48, 351–356.

Mu, X., Evans, T.D., Zhang, F., 2024. ATP biosensor reveals microbial energetic dynamics and facilitates bioproduction. Nat. Commun. 15, 5299. https://doi.org/10.1038/s41467-024-49579-1.

Novák, J., Čurdová, E., Jechová, V., Cimburková, E., Vaněk, Z., 1992. Enzymes of ammonium assimilation in Streptomyces avermitilis. Folia Microbiol. 37, 261–266. https://doi.org/10.1007/BF02814560.

Omar, H., Elsayed, E.A., Kenawy, A.A., Wadaan, M.A., El-Enshasy, H.A., 2014. Effect of cultivation scale and shear stress on cell growth and oxytetracycline production by *Streptomyces rimosus* in semi-defined medium. J. Pure Appl. Microbiol. 8 (1), 121–128.

Pérez, G. L., Vera, M. S., Miranda, L. A., (2011). Effects of Herbicide Glyphosate and Glyphosate-Based Formulations on Aquatic Ecosystems. In: Kortekamp, A. (Eds.), eBooks InTech, Herbicides and Environment, pp.343-368). Doi: 10.5772/12877.

Peter, C. P., (2006). Design of shaken bioreactors for fermentation systems with elevated viscosity and hydromechanical sensibility. Ph.D. Thesis (Thesis advisor Büchs, J.), RWTH Aachen, Germany. Publication server of RWTH Aachen University (2007). urn:nbn:de:hbz:82-opus-18570.

Porto de Souza Vandenberghe, L., Herrmann, L.W., De Oliveira Penha, R., De Mello, A.F. M., Martínez-Burgos, W.J., Magalhães, A.I., Junior, De Souza Kirnev, P.C., De Carvalho, J.C., Soccol, C.R., (2022). Engineering aspects for scale-up of bioreactors, Curr. Dev. Biotechnol. Bioeng. Adv. Bioprocess Eng., pp. 59-85, Chapter 3, in: Elsevier eBooks. Doi: 10.1016/b978-0-323-91167-2.00002-2.

Parven, A., Meftaul, I.M., Venkateswarlu, K., Megharaj, M., 2024. Herbicides in modern sustainable agriculture: environmental fate, ecological implications, and human health concerns. Int. J. Environ. Sci. Technol. 22 (2), 1181–1202. https://doi.org/10.1007/s13762-024-05818-y.

Pressley, S.R., Gonzales, J.N., Atsumi, S., 2024. Efficient utilization of xylose requires CO2 fixation in Synechococcus elongatus PCC 7942. Metab. Eng. https://doi.org/10.1016/j.ymben.2024.09.010.

Ramijan, K., Ultee, E., Willemse, J., Zhang, Z., Wondergem, J.A.J., Van der Meij, A., Heinrich, D., Briegel, A., Van Wezel, G.P., Claessen, D., 2018. Stress-induced formation of cell wall-deficient cells in filamentous actinomycetes. Nat. Commun. 9. https://doi.org/10.1038/s41467-018-07560-9.

Rapp, J., Rath, P., Kilian, J., Brilisauer, K., Grond, S., Forchhammer, K., 2021. A bioactive molecule made by unusual salvage of radical SAM enzyme byproduct 5-deoxyadenosine blurs the boundary of primary and secondary metabolism. J. Biol. Chem. 296, 100621. https://doi.org/10.1016/j.jbc.2021.100621.

Rawat, D., Bains, A., Chawla, P., Kaushik, R., Yadav, R., Kumar, A., Sridhar, K., Sharma, M., 2023. Hazardous impacts of glyphosate on human and environment health: occurrence and detection in food. Chemosphere 329, 138676. https://doi.org/10.1016/j.chemosphere.2023.138676.

Ren, F., Chen, L., Tong, Q., 2014. Influence of ammonium salt and fermentation pH on acarbose yield from streptomyces M37. Trop. J. Pharm. Res. 13 (12), 2075–2082. https://doi.org/10.4314/tjpr.v13i12.19.

Ribeiro, R.M.M.G.P., Esperança, M.N., Sousa, A.P.A., Neto, Á.B., Cerri, M.O., 2021. Individual effect of shear rate and oxygen transfer on clavulanic acid production by *Streptomyces clavuligerus*. Bioprocess Biosyst. Eng. 44, 1721–1732. https://doi.org/10.1007/s00449-021-02555-1.

Rigali, S., Titgemeyer, F., Barends, S., Mulder, S., Thomae, A.W., Hopwood, D.A., van Wezel, G.P., 2008. Feast or famine: the global regulator DasR links nutrient stress to antibiotic production by Streptomyces. EMBO Rep. 9, 670–675. https://doi.org/10.1038/embor.2008.83.

Romero-Rodríguez, A., Maldonado-Carmona, N., Ruiz-Villafán, B., Koirala, N., Rocha, D., Sánchez, S., 2018. Interplay between carbon, nitrogen and phosphate utilization in the control of secondary metabolite production in Streptomyces. Antonie Van Leeuwenhoek 111, 761–781. https://doi.org/10.1007/s10482-018-1073-1.

Rosch, T.M., Tenhaef, J., Stoltmann, T., Redeker, T., Kösters, D., Hollmann, N., Krumbach, K., Wiechert, W., Bott, M., Matamouros, S., Marienhagen, J., Noack, S., 2024. AutoBioTech–a versatile biofoundry for automated strain engineering. ACS Synth. Biol. 13, 2227–2237. https://doi.org/10.1021/acssynbio.4c00298.

Rosmine, E., Sainjan, N.C., Silvester, R., Alikkunju, A., Varghese, S.A., 2017. Statistical optimisation of xylanase production by estuarine Streptomyces sp. and its application in clarification of fruit juice. J. Genet. Eng. Biotechnol. 15, 393–401. https://doi.org/10.1016/j.jgeb.2017.06.001.

Roubos, J.A., Krabben, P., Luiten, R.G.M., Verbruggen, H.B., Heijnen, J., 2001. A quantitative approach to characterizing cell lysis caused by mechanical agitation of streptomyces clavuligerus. Biotechnol. Prog. 17 (2), 336–347. https://doi.org/10.1021/bp0001617.

Rushton, J.H. (1950). Power Characteristics of Mixing Impellers part 1.

Ruuskanen, S., Fuchs, B., Nissinen, R., Puigbò, P., Rainio, M., Saikkonen, K., Helander, M., 2022. Ecosystem consequences of herbicides: the role of microbiome. Trends Ecol. Evol. 38, 35–43. https://doi.org/10.1016/j.tree.2022.09.009.

Schweizer, M., Brilisauer, K., Triebskorn, R., Forchhammer, K., Köhler, H., 2019. How glyphosate and its associated acidity affect early development in zebrafish (Danio rerio). PeerJ, 7, e7094. https://doi.org/10.7717/peerj.7094.

Sevcikova, B., Benada, O., Kofronova, O., Kormanec, J., 2001. Stress-response sigma factor σ^H is essential for morphological differentiation of *Streptomyces coelicolor* A3 (2). Arch. Microbiol. 177, 98–106. https://doi.org/10.1007/s00203-001-0367-1.

Sevcikova, B., Kormanec, J., 2004. Differential production of two antibiotics of *Streptomyces coelicolor* A3(2), actinorhodin and undecylprodigiosin, upon salt stress conditions. Arch. Microbiol. 181, 384–389. https://doi.org/10.1007/s00203-004-0669-1.

Shao, Z.H., Ren, S.X., Liu, X.Q., Xu, J., Yan, H., Zhao, G.P., Wang, J., 2015. A preliminary study of the mechanism of nitrate-stimulated remarkable increase of rifamycin production in Amycolatopsis mediterranei U32 by RNA-seq. Microb. Cell Fact. 14, 75. https://doi.org/10.1186/s12934-015-0264-y.

Shapiro, S., Vining, L.C., 1983. Nitrogen metabolism and chloramphenicol production in *Streptomyces venezuelae*. Can. J. Microbiol. 29 (12), 1706–1714. https://doi.org/10.1139/m83-261.

Shapiro, S., Vining, L.C., 1984. Suppression of nitrate utilization by ammonium and its relationship to chloramphenicol production in *Streptomyces venezuelae*. Can. J. Microbiol. 30 (6), 798–804. https://doi.org/10.1139/m84-122.

Shapiro, S., Vining, L.C., 1985. Effect of ammonium on chloramphenicol production by *Streptomyces venezuelae* in batch and continuous cultures. Can. J. Microbiol. 31 (2), 119–123. https://doi.org/10.1139/m85-023.

Shepherd, M.D., Kharel, M.K., Bosserman, M.A., Rohr, J., (2010). Laboratory Maintenance of Streptomyces Species. Current Protocols in Microbiology, Chapter Unit–10E.1. Doi: 10.1002/9780471729259.mc10e01s18.

Shi, Z., Liu, P., Liao, X., Mao, Z., Zhang, J., Wang, Q., Sun, J., Ma, H., Ma, Y., 2022. Data-driven synthetic cell factories development for industrial biomanufacturing. BioDesign Research 2022. https://doi.org/10.34133/2022/9898461.

Shomura, T., Niwa, T., Amano, S., Yoshida, J., Moriyama, C. and Niida, T., (1970). Studies on new antibiotics, SF-666 A and B. II. Some biological characteristics of SF-666 A and B.Sci. Rep. Meiji Seika Kaisha 11: 21–25.

Smith, D.F.Q., Camacho, E., Thakur, R., Barron, A.J., Dong, Y., Dimopoulos, G., Broderick, N.A., Casadevall, A., 2021. Glyphosate inhibits melanization and increases susceptibility to infection in insects. PLoS Biol. 19 (5), e3001182. https://doi.org/10.1371/journal.pbio.3001182.

Soares, D., Silva, L., Duarte, S., Pena, A., Pereira, A., 2021. Glyphosate use, toxicity and occurrence in food. Foods 10 (11), 2785. https://doi.org/10.3390/foods10112785.

Söhnel, O., Novotny, P., 1985. Densities of Aqueous Solutions of Inorganic Substances. Elsevier, Amsterdam.

Sparks, T.C., Lorsbach, B.A., 2016. Perspectives on the agrochemical industry and agrochemical discovery. Pest Manag. Sci. 73, 672–677. https://doi.org/10.1002/ps.4457.

Stanbury, P.F., Whitaker, A., Hall, S.J., 2016. Aeration and agitation. Elsevier eBooks. 537–618. https://doi.org/10.1016/b978-0-08-099953-1.00009-0.

Taghavi, M., Zadghaffari, R., Moghaddas, J., Moghaddas, Y., 2011. Experimental and CFD investigation of power consumption in a dual Rushton turbine stirred tank. Process Saf. Environ. Prot. 89, 280–290. https://doi.org/10.1016/j.cherd.2010.07.006.

Tan, C., Xu, P., Tao, F., 2022. Carbon-negative synthetic biology: challenges and emerging trends of cyanobacterial technology. Trends Biotechnol. 40, 1488–1502. https://doi.org/10.1016/j.tibtech.2022.09.012.

Thakur, D., Bora, T.C., Bordoloi, G.N., Mazumdar, S., 2009. Influence of nutrition and culturing conditions for optimum growth and antimicrobial metabolite production by Streptomyces sp. 201. J. Mycol. Méd. 19, 161–167. https://doi.org/10.1016/j.mycmed.2009.04.001.

Tiffert, Y., Supra, P., Wurm, R., Wohlleben, W., Wagner, R., Reuther, J., 2008. The *Streptomyces coelicolor* GlnR regulon: identification of new GlnR targets and evidence for a central role of GlnR in nitrogen metabolism in actinomycetes. Mol. Microbiol. 67 (4), 861–880. https://doi.org/10.1111/j.1365-2958.2007.06092.x.

Usmani, Z., Sharma, M., Diwan, D., Tripathi, M., Whale, E., Jayakody, L.N., Moreau, B., Thakur, V.K., Tuohy, M., Gupta, V.K., 2021. Valorization of sugar beet pulp to value-added products: a review. Bioresour. Technol. 346, 126580. https://doi.org/10.1016/j.biortech.2021.126580.

Van Wezel, G.P., Krabben, P., Traag, B.A., Keijser, B.J.F., Kerste, R., Vijgenboom, E., Heijnen, J.J., Kraal, B., 2006. Unlocking streptomyces spp. for use as sustainable industrial production platforms by morphological engineering. Appl. Environ. Microbiol. 72, 5283–5288. https://doi.org/10.1128/aem.00808-06.

Wallace, K.K., Speedie, M.K., Payne, G.F. (1996). Use of Fed-Batch Operation to Improve Secondary Metabolite Production. In: Moreira, A.R., Wallace, K.K. (eds) Computer and Information Science Applications in Bioprocess Engineering. NATO ASI Series, vol 305. Springer, Dordrecht. Doi: 10.1007/978-94-009-0177-3_27.

Wang, D., Li, W., Zhang, X., Liang, S., Lin, Y., 2021. Green process: improved semi-continuous fermentation of pichia pastoris based on the principle of vitality cell separation. Front. Bioeng. Biotechnol. 9, 777774. https://doi.org/10.3389/fbioe.2021.777774.

Wang, S., Seiwert, B., Kästner, M., Miltner, A., Schäffer, A., Reemtsma, T., Yang, Q., Nowak, K.M., 2016. (Bio)degradation of glyphosate in water-sediment microcosms – a stable isotope co-labeling approach. Water Res. 99, 91–100. https://doi.org/10.1016/j.watres.2016.04.041.

Wewetzer, S.J., Kunze, M., Ladner, T., Luchterhand, B., Roth, S., Rahmen, N., Kloß, R., Silva, A.C.E., Regestein, L., Büchs, J., 2015. Parallel use of shake flask and microtiter plate online measuring devices (RAMOS and BioLector) reduces the number of experiments in laboratory-scale stirred tank bioreactors. J. Biol. Eng. 9, 9. https://doi.org/10.1186/s13036-015-0005-0.

Wolf, A. V., (1966). Aqueous Solutions and Body Fluids, Hoeber.

Yang, J., Lu, C., Stasny, B., Henley, J., Guinto, W., Gonzalez, C., Gleason, J., Fung, M., Collopy, B., Benjamino, M., Gangi, J., Hanson, M., Ille, E., 2007. Fed-batch bioreactor process scale-up from 3-L to 2,500-L scale for monoclonal antibody production from cell culture. Biotechnol. Bioeng. 98, 141–154. https://doi.org/10.1002/bit.21413.

Zacchetti, B., Andrianos, A., Van Dissel, D., De Ruiter, E., Van Wezel, G.P., Claessen, D., 2018. Microencapsulation extends mycelial viability of Streptomyces lividans 66 and increases enzyme production. BMC Biotech. 18, 13. https://doi.org/10.1186/s12896-018-0425-2.

Zhou, W., Min, M., Hu, B., Ma, X., Liu, Y., Wang, Q., Shi, J., Chen, P., Ruan, R., 2013. Filamentous fungi assisted bio-flocculation: a novel alternative technique for harvesting heterotrophic and autotrophic microalgal cells. Sep. Purif. Technol. 107, 158–165. https://doi.org/10.1016/j.seppur.2013.01.030.

Zhou, Y., Han, L.-R., He, H.-W., Sang, B., Yu, D.-L., Feng, J.-T., Zhang, X., 2018. Effects of agitation, aeration and temperature on production of a novel glycoprotein GP-1 by Streptomyces kanasenisi ZX01 and scale-up based on volumetric oxygen transfer coefficient. Molecules 23 (1), 125. https://doi.org/10.3390/molecules23010125.